Important Notice to Authors

No further publication processing will occur until we receive your response to this proof.

Attached is a PDF proof of your forthcoming article in PRB. Your article has 18 pages and the Accession Code is **BH14197**.

Please note that as part of the production process, APS converts all articles, regardless of their original source, into standardized XML that in turn is used to create the PDF and online versions of the article as well as to populate third-party systems such as Portico, Crossref, and Web of Science. We share our authors' high expectations for the fidelity of the conversion into XML and for the accuracy and appearance of the final, formatted PDF. This process works exceptionally well for the vast majority of articles; however, please check carefully all key elements of your PDF proof, particularly any equations or tables.

Figures submitted electronically as separate files containing color appear in color in the online journal. However, all figures will appear as grayscale images in the print journal unless the color figure charges have been paid in advance, in accordance with our policy for color in print (https://journals.aps.org/authors/color-figures-print).

Specific Questions and Comments to Address for This Paper

1 Please check if our changes maintain the original meaning.
2 Please provide location in Refs. [35,37,38,69,95,98,107].
Q: This reference could not be uniquely identified due to incomplete information or improper format. Please check all information and amend if applicable.

ORCIDs: Please follow any ORCID links () after the author names and verify that they point to the appropriate record for each author.

Crossref Funder Registry ID: Information about an article's funding sources is now submitted to Crossref to help you comply with current or future funding agency mandates. Crossref's Funder Registry (https://www.crossref.org/services/funder-registry/) is the definitive registry of funding agencies. Please ensure that your acknowledgments include all sources of funding for your article following any requirements of your funding sources. Where possible, please include grant and award ids. Please carefully check the following funder information we have already extracted from your article and ensure its accuracy and completeness:

Other Items to Check

- Please note that the original manuscript has been converted to XML prior to the creation of the PDF proof, as described above. Please carefully check all key elements of the paper, particularly the equations and tabular data.
- Title: Please check; be mindful that the title may have been changed during the peer-review process.
- Author list: Please make sure all authors are presented, in the appropriate order, and that all names are spelled correctly.
- Please make sure you have inserted a byline footnote containing the email address for the corresponding author, if desired. Please note that this is not inserted automatically by this journal.
- Affiliations: Please check to be sure the institution names are spelled correctly and attributed to the appropriate author(s).
- Receipt date: Please confirm accuracy.
- Acknowledgments: Please be sure to appropriately acknowledge all funding sources.
- Hyphenation: Please note hyphens may have been inserted in word pairs that function as adjectives when they occur before a noun, as in "x-ray diffraction," "4-mm-long gas cell," and "*R*-matrix theory." However, hyphens are deleted from word pairs when they are not used as adjectives before nouns, as in "emission by x rays," "was 4 mm in length," and "the *R* matrix is tested."

  Note also that Physical Review follows U.S. English guidelines in that hyphens are not used after prefixes or before suffixes: superresolution, quasiequilibrium, nanoprecipitates, resonancelike, clockwise.
- Please check that your figures are accurate and sized properly. Make sure all labeling is sufficiently legible. Figure quality in this proof is representative of the quality to be used in the online journal. To achieve manageable file size for online delivery, some compression and downsampling of figures may have occurred. Fine details may have become somewhat fuzzy, especially in color figures. The print journal uses files of higher resolution and therefore details may be sharper in print. Figures to be published in color online will appear in color on these proofs if viewed on a color monitor or printed on a color printer.
- Please check to ensure that reference titles are given as appropriate.
- Overall, please proofread the entire *formatted* article very carefully. The redlined PDF should be used as a guide to see changes that were made during copyediting. However, note that some changes to math and/or layout may not be indicated.

Ways to Respond

- ***Web:*** If you accessed this proof online, follow the instructions on the web page to submit corrections.

- ***Email:*** Send corrections to prbproofs@aptaracorp.com
  Subject: **BH14197** proof corrections
- ***Fax:*** Return this proof with corrections to +1.703.791.1217. Write **Attention:** PRB Project Manager and the Article ID, **BH14197**, on the proof copy unless it is already printed on your proof printout.

PHYSICAL REVIEW B **00**, 005400 (2022)

Generalized model for the charge transport properties of dressed quantum Hall systems

Kosala Herath [*] and Malin Premaratne [†]

Advanced Computing and Simulation Laboratory (AχL), Department of Electrical and Computer Systems Engineering, Monash University, Clayton, Victoria 3800, Australia

(Received 23 August 2021; revised 19 November 2021; accepted 20 January 2022; published xxxxxxxxxx)

We present a generalized mathematical model for predicting the transport properties of a quantum system exposed to a stationary magnetic field and a high-intensity electromagnetic field. The new formulation, which applies to two-dimensional (2D) dressed quantum Hall systems, is based on Landau quantization theory and the Floquet-Drude conductivity approach. We model our system as a two-dimensional electron gas (2DEG) that interacts with two external fields. To analyze the strong light coupling with the 2DEG, we employ the Floquet theory as a nonperturbative procedure. Moreover, the Floquet-Fermi golden rule is adopted to explore the impurity scattering effects on charge transport in disordered quantum Hall systems. We derive fully analytical expressions to describe longitudinal components in the conductivity tensor in dressed quantum Hall systems. Subsequently, we demonstrate that the conductivity characteristics of quantum Hall systems can be manipulated using strong external light. Our results align with well-established and experimentally verified theoretical descriptions for undressed systems while providing a more generalized analysis of the conductivity characteristics in quantum Hall systems. Thus our model can be applied to accurately interpret the usage of strong external radiation as a tool in nanoscale quantum devices.

DOI: 10.1103/PhysRevB.00.005400

I. INTRODUCTION

Manipulating light-matter interactions in the quantum regime paved the path for an astonishing number of useful technologies in the last century. Quantum optics, which study these interactions, have drawn research attention to the disciplines of optoelectronics [1–4], sensing [5–7], energy harvesting [8–10], quantum computing [11–13], bioinformation [14,15], and many other specialities of recent technologies [16]. The studies on quantum optics of nanostructures were generally centered on metamaterials [17,18], quantum plasmonic effects [19,20], lasers and amplifiers [21–23], and quantum cavity physics [24–26]. However, in recent years, one of the foremost aims of examining nanostructures under external radiation was understanding their electron transport characteristics [27–34].

Better understanding the fundamental mechanisms of charge transport can allow us to invent novel nanoelectronic devices and optimize their performance [35]. Most recent studies on the subject have considered the driving field as a perturbation field [30,31]. However, this assumption breaks down for systems under high-intensity illuminations [34,36]. Modeling an electromagnetic field under a perturbative formalism involves expanding the interaction terms in powers of the field intensity. At high intensities, the higher-order terms influence the physics more strongly and the basis of the perturbative treatment begins to break down. In these instances, a more accurate treatment needs to be adopted. Thus we treat the interacting fermion system and the radiation as one combined quantum system, namely dressed system [31,37,38]. Here the applied high-intensity electromagnetic field identify as the *dressing field*.

Theoretical analyses on the transport properties of dressed fermion systems were recently reported in Refs. [29,31,34]. Furthermore, in Ref. [34] a general expression for conductivity in a dressed system has been derived in a fully closed analytical form. In their study, a novel type of Green's functions, namely, four-times Green's functions were used to derive the Floquet-Drude conductivity formula. This opened the path for exploring and exploiting nanostructures' charge transport attributes under an intense dressing field.

Quantum Hall effect [39] observed in two-dimensional (2D) fermion systems at low temperatures under strong stationary magnetic fields manifest remarkable magnetotransport behaviors. Transport properties of these systems have recently attracted both theoretical [40–46] and experimental [47–49] interest. EndoÂ *et al.* [46] presented the calculations of longitudinal and transverse conductivity tensor components and their relationship in a quantum Hall system. These theoretical calculations align better with experimental observations compared to previous studies.

In contrast, we can observe more exciting phenomena by simultaneously applying a dressing field to a quantum Hall system already under a nonoscillating magnetic field. Whilst there exist several leading theories for calculating conductivity tensor elements in quantum Hall systems [41,45,46], these studies have not been utilized to describe the optical manipulation of charge transport. Recently, experimental research on the effects of microwave illumination of 2DEG systems revealed microwave-induced resistance oscillations (MIROs)

[*] kosala.herath@monash.edu
[†] malin.premaratne@monash.edu

under weak magnetic fields [50–53]. This inspired investigations on the theoretical description of MIROs and several semi-classical and quantum kinetic equation formalisms have been proposed to address the underlying mechanism of MIROs [54–57]. These formalisms provide a proper explanation for the experimental observations of MIROs. However, these experimental and theoretical works have been linked to the effects of low-frequency (microwave) electromagnetic fields that increase the longitudinal conductivity. In contrast to that, high-frequency external illumination on a 2DEG quantum Hall system leads to different behavior that reduces the longitudinal conductivity [33]. Since high-frequency radiation only contributes to the suppression of electron scattering, the driving field can be treated as a pure dressing (nonabsorbable) field [33]. Thus the influence induced by a high-frequency pure dressing field on magnetotransport properties of 2DEG quantum Hall system need to be described by a nonabsorption mechanism, and it has escaped the researchers' attention before. Lately, Dini *et al.* [33] have investigated the one-directional conductivity behavior of dressed quantum Hall system subjected to a high-frequency field. However, they have not adopted the state-of-the-art model to describe the conductivity in a quantum Hall system. The authors of Ref. [33] used the conductivity models from Refs. [41,45], and as mentioned in Endo *et al.* [46], those models predict a semi-elliptical broadening against Fermi level for each Landau level and provide less agreement with the empirical results.

In the present analysis, we introduce a robust mathematical model for a dressed two-dimensional electron gas (2DEG) subject to another nonoscillating magnetic field. A stationary magnetic field is applied perpendicularly across the surface of the 2DEG system. This causes the orbital motion of the electrons to be quantized, and a discrete energy spectrum with Landau splitting is observed [58]. It is important to note that, we limit the applied magnetic field to a range where we can neglect effects such as Anderson localization, formation of the edge states, spin splitting, and the electron-electron interactions. These are not overly restrictive assumptions, and other have successfully used same assumptions in their work, e.g., see Endo *et al.* [46]. In this study, we explicitly calculate the longitudinal components $(\sigma^{xx}, \sigma^{yy})$ of the conductivity tensor in a periodically driven quantum Hall system by developing a generalized analytical description using the Floquet-Drude conductivity [34]. Finally, we demonstrate that our generalized model reproduces the results of the state-of-the-art conductivity model in Ref. [46], which was developed for the more specific case of quantum Hall systems without the external dressing field. Moreover, we find that the optical field can be used as a mechanism to regulate transport behavior in numerous 2D nanostructures which can serve as a basis for many useful nanoelectronic devices. We believe that our theoretical analysis and visual depictions of numerical results will lead to a better understanding of manipulating charge transport. Moreover, this will inspire advanced developments in nanoscale quantum devices.

The paper is organized as follows. Section II introduces our dressed quantum Hall system and the exact wave function solutions for the given configuration. Section III provides the Floquet theory interpretation of these wave functions. We introduce the Floquet-Fermi golden rule for a quantum Hall system in Sec. IV and use it in Sec. V to derive analytical expressions for longitudinal components of conductivity. The derived theoretical model is further analyzed numerically using empirical system parameters and compared with previous studies in Sec. VI. In Sec. VII, we discuss the physical significance of our theoretical results and their possible use in future nanoelectronic devices. Finally, we summarize our findings and present our conclusions in Sec. VIII.

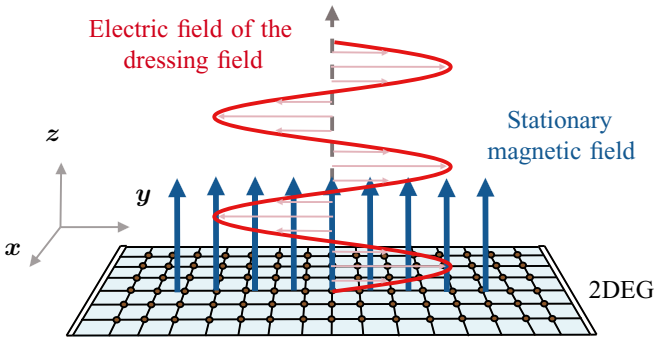

FIG. 1. Our 2DEG system only confined in the xy plane, while both of the stationary magnetic field **B** and the dressing field are applied perpendicular to the plane of 2DEG. The dressing field is linearly polarized with a y-polarized electric field **E**.

II. SCHRODINGER PROBLEM FOR A DRESSED QUANTUM HALL SYSTEM

Our system consists of a 2DEG placed on the xy plane of the three-dimensional coordinate space. In our analysis, the 2DEG is subjected to a nonoscillating magnetic field $\mathbf{B} = (0, 0, B)^\intercal$, which is pointed towards the z axis. In addition, a linearly polarized strong light is applied perpendicular to the 2DEG surface. We specially select the frequency of the dressing field ω to be in the off-resonant regime such that the field behaves as a purely dressing field. Furthermore, without limiting the generality, we choose a y-polarized electric field $\mathbf{E} = (0, E\sin(\omega t), 0)^\intercal$ for the linearly polarized dressing field as given in Fig. 1. Here B and E represent the amplitudes of the stationary magnetic field and oscillating electric field, respectively.

Using Landau gauge for the stationary magnetic field, we can represent it as a vector potential $\mathbf{A}_s = (-By, 0, 0)^\intercal$. Furthermore, we model the dynamic dressing field in the Coulomb gauge as $\mathbf{A}_d(t) = (0, [E\cos(\omega t)]/\omega, 0)^\intercal$. These vector potentials are coupled to the momentum of 2DEG as kinetic momentum [59,60]. Thus we can represent our system with a time-dependent Hamiltonian

$$\hat{H}_e(t) = \frac{1}{2m_e}\{\hat{\mathbf{p}} - e[\mathbf{A}_s + \mathbf{A}_d(t)]\}^2, \tag{1}$$

where m_e is the effective electron mass, e is the magnitude of the electron charge, and $\hat{\mathbf{p}} = (\hat{p}_x, \hat{p}_y, 0)^\intercal$ represents the canonical momentum operator for 2DEG with electron momentum $(p_x, p_y, 0)^\intercal$. The exact solutions for the time-dependent Schrödinger equation $i\hbar\, \mathrm{d}\psi/\mathrm{d}t = \hat{H}_e(t)\psi$ were already derived in Refs. [33,61,62]. Here we present them as a

set of wave functions defined by two quantum numbers (n, m)

$$\psi_{n,m}(x,y,t) = \frac{1}{\sqrt{L_x}}\chi_n(y - y_0 - \zeta(t)) \times \exp\left(\frac{i}{\hbar}\left\{-\epsilon_n t + p_x x + \frac{eE}{\omega}(y - y_0)\cos(\omega t) + m_e\dot{\zeta}(t)[y - y_0 - \zeta(t)] + \int_0^t L(\zeta,\dot{\zeta},t')\,dt'\right\}\right), \tag{2}$$

where $n \in \mathbb{Z}_0^+$ and $m \in \mathbb{Z}$. Here L_x and L_y are dimensions of the 2DEG surface, and $\hbar$ is the reduced Planck constant. The center of the cyclotron orbit on the y axis is given by $y_0 = -p_x/(eB)$ with $p_x = 2\pi\hbar m/L_x$. Moreover, χ_n are well-known eigenstate solutions for the Schrödinger equation of the stationary quantum harmonic oscillator

$$\chi_n(y) = \left(\frac{\kappa}{2^n n!\sqrt{\pi}}\right)^{1/2} e^{-\kappa^2 y^2/2}\mathcal{H}_n(\kappa y), \tag{3}$$

with eigenvalues $\epsilon_n = \hbar\omega_0[n + (1/2)]$ where $\kappa = \sqrt{m_e\omega_0/\hbar}$, $\mathcal{H}_n(\cdot)$ is the nth Hermite polynomial, and the cyclotron frequency $\omega_0 = eB/m_e$. We represent the path shift of the driven classical oscillator $\zeta(t)$ by

$$\zeta(t) = \frac{eE}{m_e(\omega_0^2 - \omega^2)}\sin(\omega t), \tag{4}$$

and we introduce $\dot{\zeta}(t) = \partial\zeta(t)/\partial t$ for the sake of notational ease. We can identify the Lagrangian of the driven classical oscillator $L(\zeta, \dot{\zeta}, t)$ as

$$L(\zeta,\dot{\zeta},t) = \tfrac{1}{2}m_e\dot{\zeta}^2(t) - \tfrac{1}{2}m_e\omega_0^2\zeta^2(t) + eE\zeta(t)\sin(\omega t). \tag{5}$$

For details of the full derivation, refer to Appendix A. The exponential phase shifts in Eq. (2) represent the influence of the stationary magnetic field and dressing field on the electron behavior of our system. Therefore, we can renormalize the magnetotransport characteristics of 2DEG by a nonoscillating magnetic field along with a dressing field.

III. FLOQUET THEORY PERSPECTIVE

Symmetry conditions often give useful insights into the behaviors of physical quantum systems. For instance, the famous Bloch analysis of electrons in quantum systems introduces a mathematical explanation for quantum systems occupying a discrete translational symmetry in the configuration space. Similarly, Floquet theory gives a mathematical formalism that can be used for translational symmetry in time rather than in space [36,63,64]. The Floquet-Drude conductivity theory was employed recently by Wackerl *et al.* [34] as a method to analyze the transport properties of quantum systems exposed to strong radiation. In their study [34], the authors have presented more accurate results than the former theoretical descriptions [30,31] for the conductivity of nanoscale systems in the presence of a dressing field. Therefore we apply the Floquet-Drude conductivity theory to analyze our 2DEG system which is subjected to both a stationary magnetic field and a dressing field.

First, we need to identify the *quasienergies* and time periodic *Floquet modes* [36] for the wave functions given in Eq. (2). By factorizing the wave function into a linearly time-dependent part and a periodic time-dependent part, we present the quasienergies with

$$\varepsilon_n = \hbar\omega_0(n + 1/2) - \Delta_\varepsilon, \tag{6}$$

which only depends on a single quantum number n. Furthermore, we can recognize the Floquet modes as

$$\phi_{n,m}(x,y,t) = \frac{1}{\sqrt{L_x}}\chi_n(y - y_0 - \zeta(t)) \times \exp\left(\frac{i}{\hbar}\left\{p_x x + \frac{eE}{\omega}(y - y_0)\cos(\omega t) + m_e\dot{\zeta}(t)[y - y_0 - \zeta(t)] + \xi\right\}\right), \tag{7}$$

with

$$\Delta_\varepsilon = \frac{e^2E^2}{4m_e(\omega_0^2 - \omega^2)} \tag{8}$$

and

$$\xi = \frac{e^2E^2(3\omega^2 - \omega_0^2)}{8m_e\omega(\omega_0^2 - \omega^2)^2}\sin(2\omega t). \tag{9}$$

For a detailed derivation, refer to Appendix B. It is important to note that these Floquet modes are time-periodic ($T = 2\pi/\omega$) functions. At resonance $\omega = \omega_0$, the energy levels occupy a continuous spectrum and the quasienergy formalism is no longer valid [65]. Therefore, in this work, we choose a dressing field frequency obeying the condition $\omega \neq \omega_0$.

Performing the Fourier transform over the confined 2D space, we obtain the momentum space (k_x, k_y) representation of Floquet modes

$$\phi_{n,m}(k_x,k_y,t) = \sqrt{L_x}\widetilde{\chi}_n(k_y - b\cos(\omega t)) \times \exp\left(i\xi - ik_y[d\sin(\omega t) + y_0]\right), \tag{10}$$

where

$$\widetilde{\chi}_n(k) = i^n\left(\frac{1}{2^n n!\sqrt{\pi}\kappa}\right)^{1/2} e^{-k^2/(2\kappa^2)}\mathcal{H}_n(k/\kappa). \tag{11}$$

Here we have introduced new parameters

$$b = \frac{eE\omega_0^2}{\hbar\omega(\omega_0^2 - \omega^2)} \tag{12}$$

and

$$d = \frac{eE}{m_e(\omega_0^2 - \omega^2)}. \tag{13}$$

Using Floquet theory, we can re-write the wave functions derived in Eq. (2) as the *Floquet states* in momentum space

$$\psi_{n,m}(k_x,k_y,t) = \exp(-i\varepsilon_n t/\hbar)\phi_{n,m}(k_x,k_y,t). \tag{14}$$

IV. INVERSE SCATTERING TIME ANALYSIS

The Floquet-Fermi golden rule was proposed in Ref. [34] as an approach to analyze the transport properties of dressed quantum systems with impurities. However, this theory has

not been applied for a dressed quantum Hall system in the previous studies. In this analysis, we use Floquet-Fermi golden rule to identify the effects induced by impurities on the magnetotransport properties. With the help of $t - t'$ formalism [34,36,66–68] and applying Floquet states derived in Eq. (14), we can derive an expression for (l, l')th element of the inverse scattering time matrix for the Nth Landau level as

$$\left(\frac{1}{\tau(\varepsilon,k_x)}\right)_N^{ll'} = \frac{\pi\hbar\varrho^2}{e^2B^2}\delta(\varepsilon-\varepsilon_N)\int_{-\infty}^{\infty} J_l\left(\frac{b\hbar}{eB}(k_x-k_1)\right)J_{l'}\left(\frac{b\hbar}{eB}(k_x-k_1)\right) \times\left|\int_{-\infty}^{\infty}\chi_N\left(\frac{\hbar}{eB}k_2\right)\chi_N\left(\frac{\hbar}{eB}(k_1-k_x-k_2)\right)dk_2\right|^2 dk_1, \tag{15}$$

where $\varrho = \eta_{\rm imp}L_x[V_{\rm imp}/\pi]^{1/2}$, ε is a given energy value, $J_l(\cdot)$ are Bessel functions of the first kind with lth integer order, and ε_N is the energy of the Nth Landau level. A more detailed derivation is given in Appendix C. We have modeled the effect caused by impurities as a single short-range perturbation potential. Analyzing the electric properties for a specific impurity distribution is a rather formidable task. We do not consider a specific impurity distribution here as it is unlikely to represent a measured impurity configuration in an experiment. Therefore, in this study, we consider the statistically averaged properties of 2DEG over impurity configurations. Furthermore, we have assumed that a group of randomly distributed impurities forms our perturbation potential under the Edwards impurity model [34,69]. Essentially, all these assumptions mean that we can write the total scattering potential in the 2DEG as a sum of uncorrelated single impurity potentials $\upsilon(\mathbf{r})$. This enables us to approximate the impurity potential as a Gaussian white noise [34,69]. Here, $\eta_{\rm imp}$ is the number of impurities in a unit area, $V_{\rm imp} = \langle|V_{k'_x,k_x}|^2\rangle_{\rm imp}$ with $V_{k'_x,k_x} = \langle k'_x|\upsilon(x)|k_x\rangle$, and $\langle x|k_x\rangle = e^{-ik_xx}$. Moreover, in this analysis, $\langle\cdot\rangle_{\rm imp}$ represents the average over the impurity disorder. In this derivation, we only considered the first order (the Born approximation) contribution from the impurity potential.

Next, we analyze the contribution of the inverse scattering time matrix elements on the transport properties of our system. Since the disorder in the system can not significantly alter the eigenenergy values of the undressed system [34], we can neglect the contribution of all off-diagonal elements in the inverse scattering time matrix. Subsequently, we consider only the central diagonal element ($l = l' = 0$) of the inverse scattering time matrix which has the largest contribution to the transport characteristics. Along with this assumption, we introduce a new parameter as the scattering-induced broadening of the Nth Landau level [33,46]

$$\Gamma_N^{00}(\varepsilon,k_x) = \hbar\left(\frac{1}{\tau(\varepsilon,k_x)}\right)_N^{00}. \tag{16}$$

We can evaluate this as

$$\Gamma_N^{00}(\varepsilon,k_x) = \frac{\pi\hbar^2\varrho^2}{e^2B^2}\delta(\varepsilon-\varepsilon_N)\int_{-\infty}^{\infty}J_0^2\left(\frac{b\hbar}{eB}(k_x-k_1)\right)\left|\int_{-\infty}^{\infty}\chi_N\left(\frac{\hbar}{eB}k_2\right)\chi_N\left(\frac{\hbar}{eB}(k_1-k_x-k_2)\right)dk_2\right|^2 dk_1. \tag{17}$$

In addition, for a scattering scenario taking place within the same Landau level, we are able to present the delta distribution of the energy by the interpretation [33]

$$\delta(\varepsilon-\varepsilon_N) \approx \frac{1}{\pi\Gamma_N^{00}(\varepsilon,k_x)}. \tag{18}$$

Subsequently, we write the central element of inverse scattering time matrix in the more compact form

$$\Gamma_N^{00}(\varepsilon,k_x) = \varrho\left[\int_{-\infty}^{\infty}J_0^2(\lambda_1(k_x-k_1))\left|\int_{-\infty}^{\infty}\widetilde{\chi}_N(\lambda_2k_2)\widetilde{\chi}_N(\lambda_2(k_1-k_2-k_x))dk_2\right|^2 dk_1\right]^{-\frac{1}{2}}, \tag{19}$$

where $\lambda_1 = \hbar b/(eB)$ and $\lambda_2 = \hbar\kappa/(eB)$. To analyze the effects of the dressing field on the scattering-induced broadening, we introduce the normalized Nth Landau level scattering-induced broadening as

$$\Lambda_N(k_x) = \frac{\Gamma_N^{00}(\varepsilon,k_x)}{\Gamma_{N=0}^{00}(\varepsilon,k_x)\big|_{E=0}}, \tag{20}$$

which we can evaluate with

$$\Lambda_N(k_x) = \left[\frac{\int_{-\infty}^{\infty}J_0^2(\lambda_1(k_x-k_1))\left|\int_{-\infty}^{\infty}\widetilde{\chi}_N(\lambda_2k_2)\widetilde{\chi}_N(\lambda_2(k_1-k_2-k_x))dk_2\right|^2dk_1}{\int_{-\infty}^{\infty}\left|\int_{-\infty}^{\infty}\widetilde{\chi}_0(\lambda_2k_2)\widetilde{\chi}_0(\lambda_2(k_1-k_2-k_x))dk_2\right|^2dk_1}\right]^{1/2}. \tag{21}$$

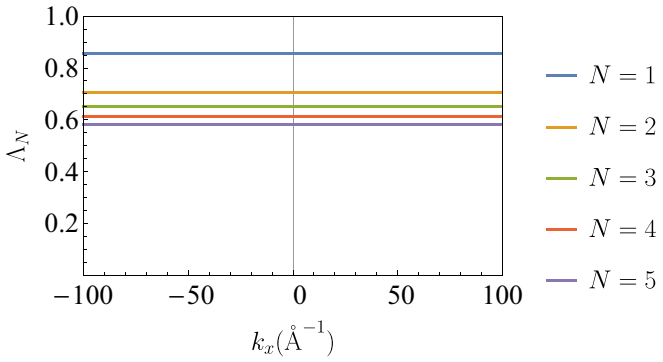

FIG. 2. The dependence of normalized scattering-induced broadening Λ_N for each Landau level ($N = 0, 1, 2, 3, 4$) against x-directional momentum value k_x in a GaAs-based quantum well under a nonoscillating magnetic field with $B = 1.2\,\text{T}$, dressing field with a frequency of $\omega = 2 \times 10^{12}\,\text{rads}^{-1}$ and intensity $I = 100\,\text{Wc}^{-2}\text{m}$. In this calculation, we have assumed that the natural broadening of zeroth Landau level Γ_0 is 0.24 meV.

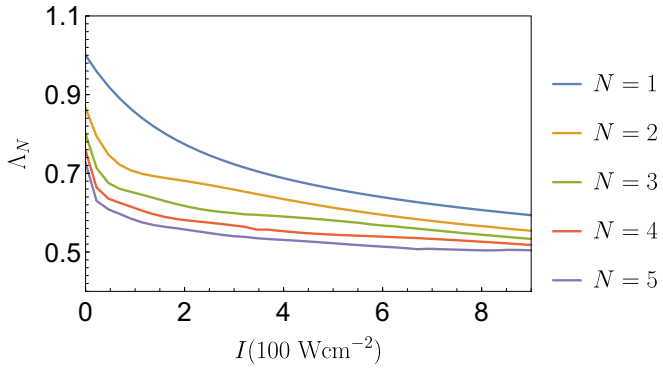

FIG. 3. The dependence of normalized scattering-induced broadening Λ_N for each Landau level ($N = 0, 1, 2, 3, 4$) against dressing field intensity I, in a GaAs-based quantum well under a nonoscillating magnetic field with $B = 1.2\,\text{T}$, dressing field with a frequency of $\omega = 2 \times 10^{12}\,\text{rads}^{-1}$. In this calculation, we have assumed that the natural broadening of zeroth Landau level Γ_0 is 0.24 meV.

Next, we calculated the normalized energy band broadening against x-directional momentum component k_x for different Landau levels ($N = 0, 1, 2, 3, 4$) for GaAs-based quantum well and the results are depicted in Figs. 2 and 3. To make a comparison, we have selected the experiment parameters to match with analysis in Ref. [46]. In the study presented in Ref. [46], the authors have assumed that the effective mass of an electron in GaAs-based quantum well system is $m_e \approx 0.07\widetilde{m}_e$, where $\widetilde{m}_e$ is the mass of the electron [34,46,70]. In addition, they used the broadening of the undressed zeroth Landau level Γ_0 as 0.24 meV. Therefore, in our calculations, we assumed that the natural least Landau level broadening also has this value: $\Gamma^{00}_{N=0}|_{E=0} = 0.24\,\text{meV}$. Here, we observe that the normalized energy broadening value for each Landau level is independent of the x-directional momentum k_x value and we are able to manipulate it by the dressing field. When the dressing field's intensity increases, the energy broadening is reduced, which leads to changes in the transport properties of the dressed quantum Hall system. To analyze these adjustments in detail, we derive an analytical expression for the conductivity of a dressed quantum Hall system in the next section.

V. FLOQUET-DRUDE CONDUCTIVITY IN A DRESSED QUANTUM HALL SYSTEM

A general theory for the conductivity of a dressed system with disorder was reported by Wackerl *et al.* [34,71]. This theory, the general x-directional longitudinal DC-limit conductivity has been characterized as

$$\sigma^{xx} = \frac{-1}{4\pi\hbar A}\int_{\Pi-\hbar\omega/2}^{\Pi+\hbar\omega/2}(-\partial f/\partial\varepsilon) \times \text{tr}\{j_0^x[\mathbf{G}^r(\varepsilon) - \mathbf{G}^a(\varepsilon)]j_0^x[\mathbf{G}^r(\varepsilon) - \mathbf{G}^a(\varepsilon)]\}d\varepsilon, \quad (22)$$

where j_0^x is the x-directional electric current operator matrix elements' zeroth Fourier component. Here, $\mathbf{G}^r(\varepsilon)$ and $\mathbf{G}^a(\varepsilon)$ are the retarded and advanced white noise disorder averaged Floquet Green function matrices [34,71], respectively, and tr{·} is the trace of the considering operators. These matrices are defined against the Floquet modes of the considering system. Here we have assumed that only zeroth Fourier component of the current operator is contributing to the conductivity. In addition, A is the area of the considered two-dimensional system, f is the partial distribution function, and Π is a function that can be chosen such that

$$\Pi - \hbar\omega/2 \leqslant \varepsilon_N < \Pi + \hbar\omega/2. \quad (23)$$

Here, ε_N are quasienergies of all relevant Floquet states.

Next, we restrict our analysis into the off-resonant regime $\omega\tau_0 \gg 1$, where τ_0 is the scattering time of the undriven system. Thus we can expand the x-directional longitudinal conductivity given in Eq. (22) using only the central entry Fourier components ($l = l' = 0$) of Floquet modes $|\phi_{n,m}\rangle = |n, k_x\rangle$ as

$$\sigma^{xx} = \frac{-1}{4\pi\hbar A}\int_{\Pi-\hbar\omega/2}^{\Pi+\hbar\omega/2}\left(-\frac{\partial f}{\partial\varepsilon}\right)\frac{1}{V_{k_x}}\sum_{k_x}\sum_{n}\langle n, k_x|j_0^x[\mathbf{G}^r(\varepsilon) - \mathbf{G}^a(\varepsilon)]j_0^x[\mathbf{G}^r(\varepsilon) - \mathbf{G}^a(\varepsilon)]|n, k_x\rangle d\varepsilon, \quad (24)$$

where V_{k_x} is the volume of considering x-directional momentum space. Next, we evaluate the above expression as follows:

$$\sigma^{xx} = \frac{-1}{4\pi\hbar A}\int_{\Pi-\hbar\omega/2}^{\Pi+\hbar\omega/2}\left(-\frac{\partial f}{\partial\varepsilon}\right)\frac{1}{V_{k_x}^4}\sum_{k_x}\sum_{n}\sum_{k_{x1},k_{x2},k_{x3}}\sum_{n_1,n_2,n_3}\langle n, k_x|j_0^x|n_1, k_{x1}\rangle\langle n_1, k_{x1}|[\mathbf{G}^r(\varepsilon) - \mathbf{G}^a(\varepsilon)] \times|n_2, k_{x2}\rangle\langle n_2, k_{x2}|j_0^x|n_3, k_{x3}\rangle\langle n_3, k_{x3}|[\mathbf{G}^r(\varepsilon) - \mathbf{G}^a(\varepsilon)]|n, k_x\rangle d\varepsilon. \quad (25)$$

We can diagonalize the impurity averaged Green's functions using a unitary transformation ($\mathbf{T} = |n, k_x\rangle$) as mentioned in Refs. [34,71,72]. Thus we evaluate the matrix elements of the difference between retarded and advanced Green's functions as

$$\langle n_1, k_{x1}|\mathbf{T}^\dagger[\mathbf{G}^r(\varepsilon) - \mathbf{G}^a(\varepsilon)]\mathbf{T}|n_2, k_{x2}\rangle = \frac{2i\Im(\mathbf{T}^\dagger\boldsymbol{\Sigma}^r\mathbf{T})\delta_{n_1,n_2}\delta_{k_{x1},k_{x2}}}{(\varepsilon/\hbar - \varepsilon_{n_1}/\hbar)^2 + [\Im(\mathbf{T}^\dagger\boldsymbol{\Sigma}^r\mathbf{T})]^2} \tag{26}$$

and

$$\langle n_3, k_{x3}|\mathbf{T}^\dagger[\mathbf{G}^r(\varepsilon) - \mathbf{G}^a(\varepsilon)]\mathbf{T}|n, k_x\rangle = \frac{2i\Im(\mathbf{T}^\dagger\boldsymbol{\Sigma}^r\mathbf{T})\delta_{n_3,n}\delta_{k_{x3},k_x}}{(\varepsilon/\hbar - \varepsilon_n/\hbar)^2 + [\Im(\mathbf{T}^\dagger\boldsymbol{\Sigma}^r\mathbf{T})]^2}. \tag{27}$$

Here we introduced the retarded self-energy matrix $\boldsymbol{\Sigma}^r$ which is the sum of all irreducible diagrams [34,71]. Applying the matrix elements of the electric current operator in Landau levels and expressions from Eqs. (26) and (27) back into Eq. (25), we obtain

$$\sigma^{xx} = \frac{-1}{4\pi\hbar A}\int_{\Pi-\hbar\omega/2}^{\Pi+\hbar\omega/2}\left(-\frac{\partial f}{\partial\varepsilon}\right)\frac{1}{V_{k_x}}\sum_{k_x}\sum_{n}\sum_{n_1,n_2}\frac{e^2B}{m_e}\left(\sqrt{\frac{n+1}{2}}\delta_{n_1,n+1} + \sqrt{\frac{n}{2}}\delta_{n_1,n-1}\right)\left\{\frac{2i\Im(\mathbf{T}^\dagger\boldsymbol{\Sigma}^r\mathbf{T})\delta_{n_1,n_2}}{(\varepsilon/\hbar - \varepsilon_{n_1}/\hbar)^2 + [\Im(\mathbf{T}^\dagger\boldsymbol{\Sigma}^r\mathbf{T})]^2}\right\}$$
$$\times\frac{e^2B}{m_e}\left(\sqrt{\frac{n_2+1}{2}}\delta_{n,n_2+1} + \sqrt{\frac{n_2}{2}}\delta_{n,n_2-1}\right)\left\{\frac{2i\Im(\mathbf{T}^\dagger\boldsymbol{\Sigma}^r\mathbf{T})}{(\varepsilon/\hbar - \varepsilon_n/\hbar)^2 + [\Im(\mathbf{T}^\dagger\boldsymbol{\Sigma}^r\mathbf{T})]^2}\right\}d\varepsilon. \tag{28}$$

For the full derivation of electric current operators in a quantum Hall system, refer to Appendix D. After the expansion, we can identify the only nonzero term as follows:

$$\sigma^{xx} = \frac{-1}{4\pi\hbar A}\frac{e^4B^2}{{m_e}^2}\int_{\Pi-\hbar\omega/2}^{\Pi+\hbar\omega/2}\left(-\frac{\partial f}{\partial\varepsilon}\right)\frac{1}{V_{k_x}}\sum_{k_x}\sum_{n}(n+1)$$
$$\times\left\{\frac{2i\Im(\mathbf{T}^\dagger\boldsymbol{\Sigma}^r(\varepsilon_{n+1},k_x)\mathbf{T})}{(\varepsilon/\hbar - \varepsilon_{n+1}/\hbar)^2 + [\Im(\mathbf{T}^\dagger\boldsymbol{\Sigma}^r(\varepsilon_{n+1},k_x)\mathbf{T})]^2}\right\}\left\{\frac{2i\Im(\mathbf{T}^\dagger\boldsymbol{\Sigma}^r(\varepsilon_n,k_x)\mathbf{T})}{(\varepsilon/\hbar - \varepsilon_n/\hbar)^2 + [\Im(\mathbf{T}^\dagger\boldsymbol{\Sigma}^r(\varepsilon_n,k_x)\mathbf{T})]^2}\right\}d\varepsilon. \tag{29}$$

The inverse scattering time matrix is equal to the diagonalized contrast of the retarded and advanced self-energy [34,71]. In addition, on the diagonal the contrast of the retarded and advanced Green's function can be represented with the imaginary component of the retarded self-energy [34,71]. Subsequently, we can identify the following property:

$$\left(\frac{1}{\tau(\varepsilon,k_x)}\right)^{ll} = -2\mathrm{Im}[\mathbf{T}^\dagger\boldsymbol{\Sigma}^r(\varepsilon,k_x)\mathbf{T}]^{ll}. \tag{30}$$

Afterwards, considering only the central element ($l = 0$) of the inverse scattering time matrix, we can restructure the derived conductivity expression in Eq. (29) as follows:

$$\sigma^{xx} = \frac{1}{\pi\hbar A}\frac{e^4B^2}{{m_e}^2}\int_{\Pi-\hbar\omega/2}^{\Pi+\hbar\omega/2}\left(-\frac{\partial f}{\partial\varepsilon}\right)\frac{1}{V_{k_x}}\sum_{k_x}\sum_{n}(n+1)\left[\frac{\widetilde{\Gamma}(\varepsilon_{n+1})}{(\varepsilon_F - \varepsilon_{n+1})^2 + \widetilde{\Gamma}^2(\varepsilon_{n+1})}\right]\left[\frac{\widetilde{\Gamma}(\varepsilon_n)}{(\varepsilon_F - \varepsilon_n)^2 + \widetilde{\Gamma}^2(\varepsilon_n)}\right]d\varepsilon, \tag{31}$$

with $\widetilde{\Gamma}(\varepsilon_n, k_x) = [\hbar/2\tau(\varepsilon_n, k_x)]^{00}$. Since we already identified that the inverse scattering time matrix's central element is independent of k_x value, we can drop the k_x-dependent in the $\widetilde{\Gamma}(\varepsilon_n, k_x)$ terms. Subsequently, we can get the sum over available momentum in x-direction. However, by considering the condition that the center of the cyclotron orbit y_0 must physically lie within the considered system, we can identify that

$$-m_e\omega_0 Ly/(2\hbar) \leqslant k_x \leqslant m_e\omega_0 Ly/(2\hbar). \tag{32}$$

To further evaluate the conductivity expression, we must specify the distribution function. Generic interacting Floquet systems absorb photons from the radiation and tend to heat [73,74]. However, a complete description of a common dressed system requires a proper treatment of photon interactions. The complexity attached to these interactions is very high. There are various strategies [74–80] for overcoming this challenge of heating and for achieving nonequilibrium steady-state distribution. Working in regimes where heating rates are strongly suppressed enables steady particle distribution function in the driven isolated quantum systems. As mentioned in Rudner *et al.* [74], placing proper conditions on energy and time scales, the distribution function of a Floquet system can be assumed to be steady. By properly selecting the frequency of the radiation, we can ensure that the interband electron transitions are controlled. This leads to significantly suppressed heating rates. Let's consider our dressed quantum Hall system under off-resonant conditions [71,74], where photon absorption does not happen. Thus we can assume that the driving field only renormalizes the system's parameters rather than changing the particle distribution function. Additionally, we can select the Fermi-Dirac distribution as our partial distribution function (f) for our Floquet system

$$f(\varepsilon) = \frac{1}{\exp[(\varepsilon - \varepsilon_F)/k_BT] + 1}, \tag{33}$$

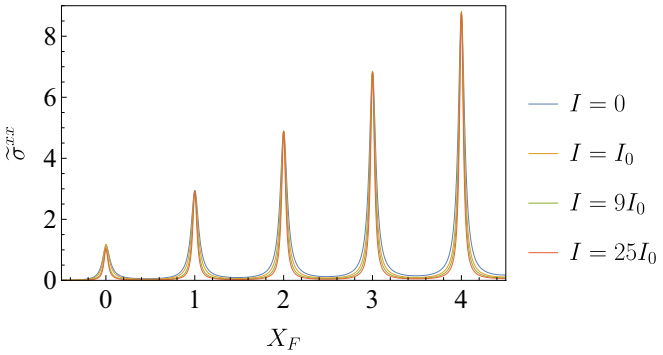

FIG. 4. Normalized longitudinal conductivity $\widetilde{\sigma}^{xx}$ against Fermi level X_F with different intensities I of the external dressing field in a GaAs-based quantum well under a nonoscillating magnetic field with $B = 1.2\,\mathrm{T}$, dressing field with a frequency of $\omega = 2 \times 10^{12}\,\mathrm{rads}^{-1}$ and $I_0 = 100\,\mathrm{Wc}^{-2}\mathrm{m}$. In this calculation, we have assumed that the natural broadening of zeroth Landau level Γ_0 is 0.24 meV.

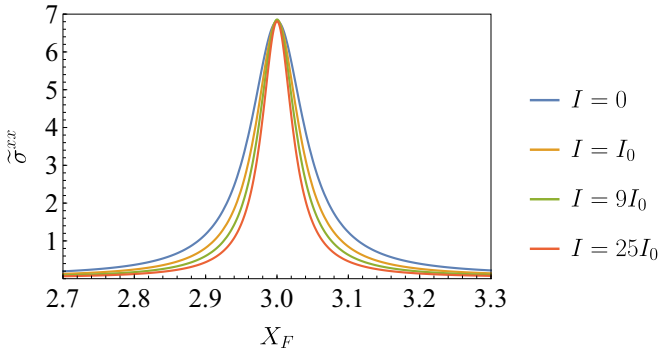

FIG. 5. Third Landau level's normalized longitudinal conductivity $\widetilde{\sigma}^{xx}$ against Fermi level X_F with different intensities I of the external dressing field in a GaAs-based quantum well under a nonoscillating magnetic field with $B = 1.2\,\mathrm{T}$, dressing field with a frequency of $\omega = 2 \times 10^{12}\,\mathrm{rads}^{-1}$ and $I_0 = 100\,\mathrm{Wc}^{-2}\mathrm{m}$. In this calculation, we have assumed that the natural broadening of zeroth Landau level Γ_0 is 0.24 meV.

where k_B is the Boltzmann constant, T is the absolute temperature, and ε_F is the Fermi energy of the system. To compare our results with the outcomes already known in the literature [33,46], we enforce the low-temperature conditions to the Fermi-Dirac distribution. At low-temperatures conditions, i.e., $k_B T \ll \varepsilon_F$, the derivative of this distribution is sharply peaked around the Fermi energy, and can be approximated by a delta function [46]

$$-\frac{\partial f(\varepsilon)}{\partial \varepsilon} \approx \delta(\varepsilon - \varepsilon_F). \tag{34}$$

Moreover, let $\Pi = \varepsilon_F$ and the derived expression in Eq. (31) leads to

$$\sigma^{xx} = \frac{e^2 l_0^2}{\pi \hbar A} \sum_n \frac{(n+1)}{\gamma_n \gamma_{n+1}} \left[\frac{1}{1 + \left(\frac{X_F - n - 1}{\gamma_{n+1}}\right)^2} \right] \times \left[\frac{1}{1 + \left(\frac{X_F - n}{\gamma_n}\right)^2} \right], \tag{35}$$

where $X_F = [\varepsilon_F/(\hbar\omega_0) - 1/2]$, $\gamma_n = \widetilde{\Gamma}(\varepsilon_n)/(\hbar\omega_0)$, and $l_0 = \sqrt{\hbar/eB}$. Following the same steps as above derivation, we can derive the longitudinal conductivity in the y direction by applying the electric current operator for y direction derived in Appendix D

$$\sigma^{yy} = \frac{e^2 l_0^2}{\pi \hbar A} \sum_n \frac{(n+1)}{\gamma_n \gamma_{n+1}} \left[\frac{1}{1 + \left(\frac{X_F - n - 1}{\gamma_{n+1}}\right)^2} \right] \times \left[\frac{1}{1 + \left(\frac{X_F - n}{\gamma_n}\right)^2} \right]. \tag{36}$$

VI. MANIPULATE CONDUCTIVITY IN QUANTUM HALL SYSTEMS

To identify the longitudinal conductivity characteristics of quantum Hall system under external dressing field, first we derive an expression for normalized longitudinal conductivity as a function of Fermi energy X_F and intensity of the dressing field I. We can identify the normalized x-directional longitudinal conductivity of dressed quantum Hall system by

$$\widetilde{\sigma}^{xx}(X_F, I) = \sigma^{xx}/\sigma_0, \tag{37}$$

with $\sigma_0 = e^2 l_0^2/(\pi \hbar A)$, and we can express this as

$$\widetilde{\sigma}^{xx}(X_F, I) = \sum_n \frac{(n+1)}{\varsigma^2 \Lambda_n \Lambda_{n+1}} \left[\frac{1}{1 + \left(\frac{X_F - n - 1}{\varsigma \Lambda_n}\right)^2} \right] \times \left[\frac{1}{1 + \left(\frac{X_F - n}{\varsigma \Lambda_{n+1}}\right)^2} \right], \tag{38}$$

where $\varsigma = \Gamma_0/(2\hbar\omega_0)$. Here, Γ_0 is the natural energy broadening of the least Landau level. The derived analytical expression is further analyzed numerically using empirical system parameters to compare with the results from previous charge transport studies on quantum Hall systems. For the interested reader, the full MATHEMATICA codes for the simulations are available in Ref. [81].

As illustrated in Figs. 4 and 5, we can manipulate the normalized longitudinal conductivity $\widetilde{\sigma}^{xx}$ with the applied dressing field's intensity and the Fermi level X_F of the considered system. For a given dressing field intensity, the longitudinal conductivity varies with the Fermi level of the system showing sharp peaks at each Landau energy level. In quantum Hall systems, electrons are restricted to bear only the Landau energies. Thus the conductivity reduces significantly when the Fermi level is not aligned with any of the Landau levels. In contrast, near each Landau level, the conductivity achieves excessive values compared to other areas. Moreover, as illustrates in Fig. 4, the peak value of the normalized longitudinal conductivity on each Landau level gets increased with the Landau level number.

By comparing the theoretical [40–46] and experimental [46,82–87] studies on the magnetoresistance of 2DEG quantum Hall systems when no radiation is present against our results, we can identify that longitudinal conductivity oscillations in Fig. 4 are a repetition of the Shubnikov–de Haas(SdH)

oscillations. As observed in the experimental work of Caviglia *et al.* [87], the period of SdH oscillations depends only on the perpendicular component of the magnetic field to the plane of the 2DEG. Therefore we can identify that many experiments on different types of 2DEGs at low-temperatures [46,83–87] have analyzed these SdH oscillations against the applied magnetic field's amplitude. The cyclotron frequency (ω_0) of the system depends on the magnetic field's perpendicular component to the plane of the 2DEG. The gate voltage modifies the Fermi level of the system. Since the Landau level energy is only dependent on the cyclotron frequency, this gate voltage variation under a constant magnetic field amplitude generates the same SdH oscillations. Interestingly, this oscillatory behavior against applied gate voltage has been observed experimentally by Wakabayashi *et al.* [82] in an inversion layer on a silicon surface at low temperature. By comparing these observations against our results in Fig. 4, we can identify that our oscillations also show the same characteristic behavior; i.e $\hbar\omega_0$ periodic SdH oscillations against the Fermi energy. Furthermore, when we increase the gate voltage, the Fermi level rises. As illustrated in Fig. 4, this will result in a higher conductivity peak value at the higher-order Landau levels. This same behavior was also observed in the experimental observations presented in Ref. [82]. In our work, we provide analytical results describing the controllability of these conductivity regions using a dressing field.

Considering the effects of the applied dressing field on the longitudinal conductivity of 2DEG, we can identify that the dressing field has sharpened the conductivity peaks. When we increase the intensity level of the dressing field, the conductivity regions get weakened as illustrated in the Fig. 5. However, the peak value of the conductivity at each Landau level has the same value as the undressed system. This demonstrates our ability to tune the width of the conductivity regions in these quantum Hall systems with the help of a dressing field.

These characteristics align well with the outcomes demonstrated by Dini *et al.* [33]. However, we can distinguish that the shapes and behavior of the conductivity regions that illustrated in Figs. 4 and 5 are generally incompatible with the results reported in Ref. [33]. This is due to the selection of the conventional longitudinal conductivity theory of 2DEG from Refs. [41,45]. The semi-elliptical conductivity regions are illustrated in Refs. [33,41,45], have less consistency with the experimentally observed data for Landau levels [46]. In our study of the transport properties of quantum Hall systems, we developed the conductivity expression starting from the Floquet-Drude conductivity [34] and we achieved outcomes that align with the results depicted in Ref. [46]. The theory on the conductivity of quantum Hall systems in Ref. [46] provides an excellent agreement with the experimentally observed results in GaAs/AlGaAs 2DEG for the low magnetic field range. However, they have not considered the tunability that can be achieved with a dressing field. In this analysis, we account for both the magnetic and dressing field effects that can affect the transport properties of 2DEG, leading to a more generalized theory. Thus, in this study, we were able to demonstrate that using Floquet-Drude conductivity method, one can derive a more generalized mathematical model which fits better with experiment for the charge transport properties of quantum Hall systems.

Lately, several experimental [50–53] and theoretical [54–57] studies have uncovered various remarkable magneto-transport properties induced by microwave radiation on 2DEG quantum Hall systems. However, these experiments and theoretical models only analyzed the behavior of MIROs in 2DEG systems which are based on low-frequency fields. It is important to state that the difference between our SdH oscillations and MIROs [50–53] by considering the frequency range of the applied electromagnetic field. In our case, the applied dressing field is in the high-frequency regime where we can neglect the photon interactions. The only influence of the electromagnetic field is the suppression of electron scattering. This will clearly describe the crucial difference between low-frequency illumination and high-frequency illumination effects on 2DEG quantum Hall systems. Therefore our theoretical analysis can help to fill the gap in knowledge of the high-frequency dressing field effects on 2DEG quantum Hall systems.

VII. PHYSICAL SIGNIFICANCE OF THE OUTCOMES

With the realization of 2DEGs in Si-MOSFETs (metal oxide semiconductor field effect transistors) [88], Klitzing *et al.* [89] made the first transport measurements on such systems to reveal the quantum Hall effect. The empirical discovery of these unusual properties marked the beginning of a whole new realm in condensed matter physics that continues to produce phenomenal advancements in electronic systems. The quantum Hall effects in a 2DEG under a static magnetic field are described by plateaus quantized to integer values of the conductivity quantum ($e^2/\hbar$) in the off-diagonal conductivity, with simultaneous peaks at inter-plateau transition for the diagonal conductivity [46]. This is due to the applied magnetic field and it changes the energy spectrum of 2DEG dramatically. The magnetic field causes the density of states in 2DEG to split up into a sequence of delta functions, separated by an energy $\hbar\omega_0$, with ω_0 the cyclotron frequency which depends on the applied magnetic field. However, experimental results demonstrate that these Landau levels are broadened and the main source of these broadening at low temperatures is the disorders in materials [90,91]. The broaden sequence of delta functions of the density of states implies the oscillating behavior in the experimental measurements of longitudinal conductivity which is known as SdH oscillations [46,82].

Our theoretical analysis on longitudinal conductivity behavior of dressed quantum Hall system was developed by considering low-temperature limit with Gaussian impurity broadening assumptions. As illustrated in Fig. 4, we can describe the experimentally observed SdH oscillation results in Refs. [46,82] through our model. Under the undressed condition, our results overlap with the conductivity measurement of quantum Hall systems [46]. Strikingly, we show in Fig. 5 that we can manipulate the broadening of these conductivity peaks using an external dressing field. At low temperatures, the principal cause of broadening of these conductivity peaks is impurity-induced scattering. Using an external dressing field, we can suppress the impurity-induced scattering and this results a reduction of both the scattering-induced broadening and the longitudinal conductivity peaks.

Research on novel states of matter has driven the evolution of present-day nanoelectronic devices. In particular,

controllable manipulation of material properties through a gate electric field has revolutionized the development of material science and technology [92,93]. The charge carrier concentration of a system is an imperative parameter that defines its conductivity properties. As we can manipulate the charge carrier concentration using an electrostatic field effect, we exert significant control over the conductivity externally. A 2DEG under static magnetic field with quantum Hall effects is an excellent example that illustrates how the gate electric field controls conductivity. We also observed that a considerable number of studies exist on charge transport in the quantum limit that employed different types of 2D field-effect transistors (FETs) subjected to magnetic fields [82,94–96]. Yang *et al.* [94] study shows quantized Hall plateaus and SdH oscillations for longitudinal conductivity against gate voltage in black phosphorus FET under static magnetic fields at low temperatures. Since the Fermi level of a system can be altered with the applied gate voltage, our Fig. 4 depicts this result. In particular, our analysis shows that we can manipulate the broadening of the conductivity regions using an external dressing field. Although Yang *et al.* [94], achieved broadening in longitudinal conductivity peaks by changing the temperature in a low range, in this study we presented a general theory on manipulating longitudinal conductivity broadening using a high-intensity electromagnetic field.

The realization of the underlying mechanism of 2D FETs in the quantum realm promises its potential in next-generation nanoelectronic applications. In a particular application that uses the switching mechanism of the above-discussed FETs with quantum Hall effects, we can achieve high and low output conductivities by changing the input gate voltage. As a result of manipulating the broadening of conductivity regions, we can limit the broadening of conductivity peaks around Landau levels using a dressing high-intensity electromagnetic field. This will enhance the sensitivity of FETs which provides the ability to observe narrow changes in gate voltage. Furthermore, adopting the mechanism presented in Ref. [97], we can manipulate conductivity peaks into very sensitive, narrowband high-frequency radiation detectors. We envision these advances in nanoelectronics from our theoretical model and knowledge generated from the insight it provides to the underlying dependencies. Furthermore, this theoretical model will aid in the development of simulation tools that will design the quantum effects in magnetotransport properties of 2D nanostructures.

VIII. CONCLUSIONS

In this paper, we introduced a generalized mathematical model for predicting charge transport properties in a 2DEG under a nonoscillating magnetic field and a high-intensity light. Under the uniform magnetic field, the charged particles can only settle in discrete energy values, which leads to the Landau quantization. We modeled the behavior of electrons in Landau levels under the dressing field utilizing the Floquet-Drude conductivity method. We modeled the impurities in the material as a Gaussian random scattering potential, and restricted the applied magnetic field to a range where we can neglect effects of Anderson localization, formation of the edge states, spin splitting, and electron-electron interactions. Finally, we derived analytical expressions for the diagonal components of electric conductivity tensor concerning the 2DEG quantum Hall system under low temperatures.

Our derived analytical expressions disclosed that we are able to control the transport characteristics of the dressed quantum Hall system by the applied dressing field's intensity. Using detailed numerical calculations with empirical system parameters, we further analyzed the manipulation of conductivity components using the dressing field. We found that the graphical illustrations that we obtained from these numerical calculations are capable of producing the same behavior as experiments on quantum Hall systems in the absence of a dressing field. Furthermore, we identified that by increasing the intensity of the radiation, we can squeeze the conductivity regions near the Landau levels. Despite this behavior being identified in the previous work of Dini *et al.* [33], they cannot fully account for the experimental observations of longitudinal conductivity components in undressed quantum Hall systems presented in Ref. [46]. The authors of Ref. [33] have used the conventional expression of longitudinal conductivity from Refs. [41,45] and this theory yields a semi-elliptical broadening for the Landau levels. These predictions significantly deviate from the experimentally observed Landau level broadening [46]. However, our generalized analysis on the conductivity of dressed quantum Hall systems provides a well-suited description for empirically observed behaviors of undressed quantum Hall systems as well.

In summary, the primary purpose of this study was to broaden the modern descriptions on transport properties of dressed quantum Hall systems. Moreover, our detailed theoretical analysis showed that we can adapt the recently introduced Floquet-Drude conductivity model to extend the models that were used to describe the transport characteristics in quantum Hall systems. Owing to the ability to control the conductivity regions, high intensity external illumination may be used as a trigger for two-dimensional quantum switching devices, which are employed as the building blocks of next-generation nanoelectronic devices. As a concluding remark, we believe that our findings of this paper can be used towards understanding the 2D optoelectronic nanotransistors, enhancing their performance, and inventing novel appliances.

ACKNOWLEDGMENTS

K.H wish to acknowledge the members of AχL at Monash University for their encouragement and support and specially T.N. Perera and R.T. Wijesekara for insightful discussions. The work of K.H is supported by the Australian Government Research Training Program (RTP) Scholarship and the Monash University Institute of Graduate Research.

APPENDIX A: WAVE-FUNCTION SOLUTIONS FOR A DRESSED QUANTUM HALL SYSTEM

The derivation of the solutions for the time-dependent Schrödinger equation with our system's Hamiltonian (1) is quite similar to that followed in Refs. [33,61]. We start with expanding the Hamiltonian for two-dimensional scenario

$$\hat{H}_e(t) = \frac{1}{2m_e}\left\{(\hat{p}_x + eBy)^2 + \left[\hat{p}_y - \frac{eE}{\omega}\cos(\omega t)\right]^2\right\}. \quad \text{(A1)}$$

Since $[\hat{H}_e(t), \hat{p}_x] = 0$, both of these operators share same eigenfunctions $L_x{}^{-1/2}\exp(ip_x x/\hbar)$ where $p_x = 2\pi\hbar m/L_x$ with $m \in \mathbb{Z}$. Thus we rearrange the Hamiltonian using the definition of canonical momentum in y direction and this leads to

$$\hat{H}_e(t) = \frac{1}{2m_e}\left\{(p_x + eBy)^2 + \left[i\hbar\frac{\partial y}{\partial -}\frac{eE}{\omega}\cos(\omega t)\right]^2\right\}. \quad \text{(A2)}$$

Subsequently, we define the *center of the cyclotron orbit* on the y-axis as $y_0 = -p_x/(eB)$, and the *cyclotron frequency* as $\omega_0 = eB/m_e$. This leads to a new arrangement of the Hamiltonian

$$\hat{H}_e(t) = \frac{m_e\omega_0^2}{2}\tilde{y}^2 + \frac{1}{2m_e}\left[-\hbar^2\frac{\partial^2}{\partial\tilde{y}^2} + \frac{2i\hbar eE}{\omega}\cos(\omega t)\frac{\partial}{\partial\tilde{y}} + \frac{e^2E^2}{\omega^2}\cos[2](\omega t)\right], \quad \text{(A3)}$$

where we used a variable substitution $\tilde{y} = (y - y_0)$. Furthermore, we assume that the wave function solutions for the time-dependent Schrödinger equation of considered quantum system

$$i\hbar\frac{d\psi}{dt} = \hat{H}_e(t)\psi, \quad \text{(A4)}$$

can be presented by the following form:

$$\psi_m(x, \tilde{y}, t) = \frac{1}{\sqrt{L_x}}\exp\left(\frac{ip_x x}{\hbar} + \frac{ieE\tilde{y}}{\hbar\omega}\cos(\omega t)\right)\vartheta(\tilde{y}, t), \quad \text{(A5)}$$

where $\vartheta(\tilde{y}, t)$ is a function that satisfy the property

$$\left[\frac{m_e\omega_0^2}{2}\tilde{y}^2 - eE\tilde{y}\sin(\omega t) - \frac{\hbar^2}{2m_e}\frac{\partial^2}{\partial\tilde{y}^2} - i\hbar\frac{d}{dt}\right]\vartheta(\tilde{y}, t) = 0. \quad \text{(A6)}$$

If we turn off the dressing field ($E = 0$), this equation leads to the Schrödinger equation with the simple harmonic oscillator Hamiltonian

$$i\hbar\frac{d\vartheta(\tilde{y}, t)}{dt} = \left(\frac{\hat{p}_{\tilde{y}}^2}{2m_e} + \frac{1}{2}m_e\omega_0^2\tilde{y}^2\right)\vartheta(\tilde{y}, t). \quad \text{(A7)}$$

Thus we can identify $S(t) = eE\sin(\omega t)$ term as an external force that act on the harmonic oscillator, and we can solve Eq. (A6) as a forced harmonic oscillator on $\tilde{y}$ axis

$$i\hbar\frac{d\vartheta(\tilde{y}, t)}{dt} = \left[-\frac{\hbar^2}{2m_e}\frac{\partial^2}{\partial\tilde{y}^2} + \frac{1}{2}m_e\omega_0^2\tilde{y}^2 - \tilde{y}S(t)\right]\vartheta(\tilde{y}, t). \quad \text{(A8)}$$

This system is exactly solvable, and we can solve the equation using the methods explained by Husimi [61]. We introduce a time-dependent shifted coordinate $y' = \tilde{y} - \zeta(t)$ and perform the following unitary transformation:

$$\vartheta(y', t) = \exp\left(\frac{im_e\dot{\zeta}y'}{\hbar}\right)\varphi(y', t), \quad \text{(A9)}$$

and this leads to

$$i\hbar\frac{\partial\varphi(y', t)}{\partial t} = \left\{-\frac{\hbar^2}{2m_e}\frac{\partial^2}{\partial y'^2} + \frac{1}{2}m_e\omega_0^2 y'^2 - \frac{1}{2}m_e\dot{\zeta}^2 + \frac{1}{2}m_e\omega_0^2\zeta^2 - \zeta S(t) + [m_e\ddot{\zeta} + m_e\omega_0^2\zeta - S(t)]y'\right\}\varphi(y', t). \quad \text{(A10)}$$

Here, we introduced $\dot{\zeta} = \partial\zeta/\partial t$ and $\ddot{\zeta} = \partial^2\zeta/\partial t^2$ for the sake of notational convenience. Subsequently, we can restrict $\zeta(t)$ function such that

$$m_e\ddot{\zeta} + m_e\omega_0^2\zeta = S(t), \quad \text{(A11)}$$

and that simply our previous expression as

$$i\hbar\frac{\partial\varphi(y', t)}{\partial t} = \left[-\frac{\hbar^2}{2m_e}\frac{\partial^2}{\partial y'^2} + \frac{1}{2}m_e\omega_0^2 y'^2 - L(\zeta, \dot{\zeta}, t)\right]\varphi(y', t). \quad \text{(A12)}$$

Here

$$L(\zeta, \dot{\zeta}, t) = \tfrac{1}{2}m_e\dot{\zeta}^2 - \tfrac{1}{2}m_e\omega_0^2\zeta^2 + \zeta S(t), \quad \text{(A13)}$$

is the Lagrangian of a classical driven oscillator. To proceed further, we introduce another unitary transform as follows:

$$\varphi(y', t) = \exp\left(\frac{i}{\hbar}\int_0^t L(\zeta, \dot{\zeta}, t')dt'\right)\chi(y', t), \quad \text{(A14)}$$

and subtitling Eq. (A14) back in Eq. (A12), we can obtain

$$i\hbar\frac{\partial}{\partial t}\chi(y', t) = \left(-\frac{\hbar^2}{2m_e}\frac{\partial^2}{\partial y'^2} + \frac{1}{2}m_e\omega_0^2 y'^2\right)\chi(y', t). \quad \text{(A15)}$$

This is the well-known Schrödinger equation of the quantum harmonic oscillator. This allows us to identify the well known eigenfunction solutions [98,99]

$$\chi_n(y) = \sqrt{\frac{\kappa}{2^n n!\sqrt{\pi}}}e^{-\kappa^2 y^2/2}\mathcal{H}_n(\kappa y), \quad \text{(A16)}$$

with eigenvalues

$$\epsilon_n = \hbar\omega_0\left(n + \frac{1}{2}\right) \text{ for } n \in \mathbb{Z}_0^+. \quad \text{(A17)}$$

Here, $\kappa = \sqrt{m_e\omega_0/\hbar}$, and $\mathcal{H}_n$ are the Hermite polynomials. Thus we can identify the solutions for Eq. (A8) as

$$\vartheta_n(\tilde{y}, t) = \chi_n(\tilde{y} - \zeta(t))\exp\left(\frac{i}{\hbar}\left\{-\epsilon_n t + m_e[\tilde{y} - \zeta(t)]\dot{\zeta}(t) + \int_0^t L(\zeta, \dot{\zeta}, t')dt'\right\}\right). \quad \text{(A18)}$$

Since $\chi_n(x)$ functions forms a complete set, we can present any general solution for $\vartheta(\tilde{y}, t)$ using the solutions derived in Eq. (A18).

Finally, we consider our scenario where we can assume that $S(t) = eE\sin(\omega t)$, and we can derive the solution for Eq. (A11) as

$$\zeta(t) = \frac{eE}{m_e(\omega_0^2 - \omega^2)}\sin(\omega t). \quad \text{(A19)}$$

Substituting solutions given in Eq. (A18) back in Eq. (A5), we obtain a set of wave functions with two different quantum number (n, m) that satisfy the time-dependent Schrödinger

equation Eq. (A4) as follows:

$$\psi_{n,m}(x,y,t) = \frac{1}{\sqrt{L_x}}\chi_n(y-y_0-\zeta(t)) \times \exp\left(\frac{i}{\hbar}\left\{-\epsilon_n t + p_x x + \frac{eE(y-y_0)}{\omega}\cos(\omega t) + m_e[y-y_0-\zeta(t)]\dot{\zeta}(t) + \int_0^t L(\zeta,\dot{\zeta},t')dt'\right\}\right). \tag{A20}$$

APPENDIX B: FLOQUET MODES AND QUASIENERGIES

1. Position space representation

First we define the time integral of the Lagrangian of the classical oscillator given in Eq. (5), over a period $T = 2\pi/\omega$ as

$$\Delta_\varepsilon = \frac{1}{T}\int_0^T L(\zeta,\dot{\zeta},t')dt'. \tag{B1}$$

Additionally, performing this integral, we can obtain a more simplified result

$$\Delta_\varepsilon = \frac{e^2E^2}{4m_e\left(\omega_0^2-\omega^2\right)}. \tag{B2}$$

Next, we define another parameter

$$\xi = \int_0^t L(\zeta,\dot{\zeta},t')dt' - \Delta_\varepsilon t, \tag{B3}$$

and after simplifying, we can identify

$$\xi = \frac{e^2E^2\left(3\omega^2-\omega_0^2\right)}{8m_e\omega\left(\omega_0^2-\omega^2\right)^2}\sin(2\omega t), \tag{B4}$$

which is a periodic function in time. Using these parameters, we can factorize the wave function given in Eq. (2) as linearly time-dependent part and periodic time-dependent part as follows:

$$\psi_\alpha(x,y,t) = \exp\left(\frac{i}{\hbar}(-\epsilon_n t + \Delta_\varepsilon t)\right)\frac{1}{\sqrt{L_x}}\chi_n(y-y_0-\zeta(t)) \times \exp\left(\frac{i}{\hbar}\left\{p_x x + \frac{eE(y-y_0)}{\omega}\cos(\omega t) + m_e\dot{\zeta}(t)[y-y_0-\zeta(t)] + \xi\right\}\right). \tag{B5}$$

This leads to separate the linear time-dependent phase component as the quasienergies

$$\varepsilon_n = \hbar\omega_0\left(n+\frac{1}{2}\right) - \Delta_\varepsilon, \tag{B6}$$

while rest of the components as time-periodic Floquet modes

$$\phi_{n,m}(x,y,t) = \frac{1}{\sqrt{L_x}}\chi_n(y-y_0-\zeta(t)) \times \exp\left(\frac{i}{\hbar}\left\{p_x x + \frac{eE(y-y_0)}{\omega}\cos(\omega t) + m_e\dot{\zeta}(t)[y-y_0-\zeta(t)] + \xi\right\}\right). \tag{B7}$$

2. Momentum space representation

We perform continuous Fourier transform over the considering confined space $A = L_xL_y$ on the Floquet modes given in Eq. (7) to realize the Floquet modes in momentum space

$$\phi_{n,m}(k_x,k_y,t) = \exp\left(\frac{-i\gamma(t)}{\hbar}y_0\right)\exp\left(\frac{-i}{\hbar}\left[m_e\dot{\zeta}(t)\zeta(t)-\xi\right]\right) \times \int_{-L_y/2}^{L_y/2}\exp(-i[k_y-\gamma(t)]y)\chi_n(y-\mu(t))dy \times \frac{1}{\sqrt{L_x}}\int_{-L_x/2}^{L_x/2}\exp(-ik_x x)\exp(ip_x/\hbar x)dx. \tag{B8}$$

Here we used new two parameters

$$\mu(t) = \frac{eE\sin(\omega t)}{m_e\left(\omega_0^2-\omega^2\right)} + y_0 \tag{B9}$$

and

$$\gamma(t) = \frac{eE\omega_0^2\cos(\omega t)}{\hbar\omega\left(\omega_0^2-\omega^2\right)}. \tag{B10}$$

Subsequently, using the Fourier transform identity [60]

$$\int_{-L_x/2}^{L_x/2}\exp(-ik_x x + ip_x x/\hbar)dx = L_x\delta_{k_x,p_x/\hbar}, \tag{B11}$$

we can derive

$$\phi_{n,m}(k_x,k_y,t) = \Phi_{n,m}(k_y,t)\delta_{k_x,p_x/\hbar}\exp\left(\frac{-i}{\hbar}\gamma(t)y_0\right) \times \exp\left(\frac{-i}{\hbar}[m_e\dot{\zeta}(t)\zeta(t)-\xi]\right), \tag{B12}$$

where we can define $\Phi_{n,m}(k_y,t)$ as

$$\Phi_{n,m}(k_y,t) = \sqrt{L_x}\int_{-L_y/2}^{L_y/2}\chi_n(y-\mu(t))\exp\left(-i[k_y-\gamma(t)]y\right)dy. \tag{B13}$$

Substituting $k_y' = k_y - \gamma(t)$ with $y' = y - \mu(t)$, and assuming that the size of the considered 2DEG sample in y-direction is considerably large ($L_y \to \infty$), we can obtain

$$\Phi_{n,m}(k_y',t) = \sqrt{L_x}e^{-ik_y'\mu}\int_{-\infty}^{\infty}\chi_n(y')\exp(-ik_y'y')dy'. \tag{B14}$$

Moreover, we can identify that the above integral represents the Fourier transform of χ_n functions. In addition, using the symmetric conditions of the Fourier transform for Gauss-Hermite functions $\theta_n(x)$ [100]

$$\mathcal{FT}[\theta_n(\kappa x),x,k] = \frac{i^n}{|\kappa|}\theta_n(k/\kappa), \tag{B15}$$

we can simply the Eq. (B14) as

$$\Phi_{n,m}(k_y',t) = \sqrt{L_x}e^{-ik_y'\mu}\widetilde{\chi}_n(k_y'), \tag{B16}$$

with

$$\widetilde{\chi}_n(k) = \frac{i^n}{\sqrt{2^n n!\sqrt{\pi}}}\left(\frac{1}{\kappa}\right)^{1/2}e^{-k^2/(2\kappa^2)}\mathcal{H}_n(k/\kappa). \tag{B17}$$

Finally, substitute Eq. (B16) back into Eq. (B12) and this leads to

$$\phi_{n,m}(k_x,k_y,t) = \sqrt{L_x}\widetilde{\chi}_n(k_y - b\cos(\omega t)) \times \exp\left(i\xi - ik_y\left[d\sin(\omega t) + \frac{\hbar k_x}{eB}\right]\right), \tag{B18}$$

where

$$b = \frac{eE\omega_0^2}{\hbar\omega\left(\omega_0^2 - \omega^2\right)} \tag{B19}$$

and

$$d = \frac{eE}{m_e\left(\omega_0^2 - \omega^2\right)}. \tag{B20}$$

It is necessary to notice that k_x is quantized with $k_x = 2\pi m/L_x,\ m \in \mathbb{Z}$.

APPENDIX C: FLOQUET-FERMI GOLDEN RULE FOR A DRESSED QUANTUM HALL SYSTEM

We derive the Floquet-Fermi golden rule for our dressed quantum Hall system with the help of the t-t' formalism. The t-t'-Floquet states [34,36]

$$|\psi_{n,m}(t,t')\rangle = \exp\left(-\frac{i}{\hbar}\varepsilon_n t\right)|\phi_{n,m}(t')\rangle \tag{C1}$$

are derived by separating the aperiodic and periodic components of the Floquet states given in Eq. (14). Additionally, these states fulfill the t-t'-Schrödinger equation [34,36]

$$i\hbar\frac{\partial}{\partial t}|\psi_{n,m}(t,t')\rangle = H_F(t')|\psi_{n,m}(t,t')\rangle, \tag{C2}$$

where the *Floquet Hamiltonian* defined as

$$H_F(t') = H_e(t') - i\hbar\frac{\partial}{\partial t'}. \tag{C3}$$

Next, we can identify the time evolution operator corresponding to the t-t'-Schrödinger equation as

$$U_F(t,t_0;t') = \exp\left(-\frac{i}{\hbar}H_F(t')[t-t_0]\right). \tag{C4}$$

The advantage of the t-t' formalism lies on this time evolution operator, which avoids any time ordering operators [34].

We model the effect caused by impurities in the considered system as a single perturbation potential formed by a group of randomly distributed impurities. Thus we introduce a time-independent total perturbation $V(\mathbf{r})$ which has been turned on at the reference time $t = t_0$, and the t-t'-Schrödinger equation becomes

$$i\hbar\frac{\partial}{\partial t}|\Psi_{n,m}(t,t')\rangle = [H_F(t') + V(\mathbf{r})]|\Psi_{n,m}(t,t')\rangle. \tag{C5}$$

This introduces a new wave function solution $|\Psi_{n,m}\rangle$ for a system with a given perturbation. If $t \leqslant t_0$, both of the solutions for Eqs. (C2) and (C5) coincide

$$|\psi_{n,m}(t,t')\rangle = |\Psi_{n,m}(t,t')\rangle \quad \text{when} \quad t \leqslant t_0. \tag{C6}$$

Next, we move our analysis into the interaction picture representation [59,60] and in the interaction picture, we can identify the t-t'-Floquet state as

$$|\Psi_{n,m}(t,t')\rangle_I = U_0^\dagger(t,t_0;t')|\Psi_{n,m}(t,t')\rangle. \tag{C7}$$

Due to time independence, the perturbation in the interaction picture has the same form as the Schrödinger picture representation

$$V_I(\mathbf{r}) = U_0^\dagger(t,t_0;t')V(\mathbf{r})U_0(t,t_0;t') = V(\mathbf{r}). \tag{C8}$$

This leads us to the t-t'-Schrödinger equation in the interaction picture representation

$$i\hbar\frac{\partial}{\partial t}|\Psi_{n,m}(t,t')\rangle_I = V_I(\mathbf{r})|\Psi_{n,m}(t,t')\rangle_I, \tag{C9}$$

with the recursive solutions [59,60]

$$|\Psi_{n,m}(t,t')\rangle_I = |\Psi_{n,m}(t_0,t')\rangle_I + \frac{1}{i\hbar}\int_{t_0}^{t} V_I(\mathbf{r})|\Psi_{n,m}(t_1,t')\rangle_I dt_1. \tag{C10}$$

Iterating the solution only up to the first order (Born approximation), we obtain

$$|\Psi_{n,m}(t,t')\rangle_I \approx |\psi_{n,m}(t_0,t')\rangle + \frac{1}{i\hbar}\int_{t_0}^{t} V_I(\mathbf{r})|\psi_{n,m}(t_0,t')\rangle dt_1. \tag{C11}$$

Since our t-t'-Floquet states create a basis, we can represent the solutions for the t-t'-Schrödinger equation given in Eq. (C5) using our known t-t'-Floquet states as follows:

$$|\Psi_\alpha(t,t')\rangle = \sum_\beta a_{\alpha,\beta}(t,t')|\psi_\beta(t,t')\rangle. \tag{C12}$$

Here, we used a single term notation to represent two quantum numbers; $\alpha \equiv (n_\alpha, m_\alpha)$ and $\beta \equiv (n_\beta, m_\beta)$. Subsequently, we can identify the *scattering amplitude* as $a_{\alpha,\beta}(t,t') = \langle\psi_\beta(t,t')|\Psi_\alpha(t,t')\rangle$ and we can evaluate this with

$$a_{\alpha,\beta}(t,t') = \langle\psi_\beta(t,t')|\psi_\alpha(t,t')\rangle + \frac{1}{i\hbar}\int_{t_0}^{t}\langle\psi_\beta(t_1,t')|V(\mathbf{r})|\psi_\alpha(t_1,t')\rangle dt_1. \tag{C13}$$

Since the t-t'-Floquet states are orthonormal and assuming $t_0 = 0$ and $\alpha \neq \beta$ this leads to

$$a_{\alpha,\beta}(t,t') = -\frac{i}{\hbar}\int_0^t \langle\psi_\beta(t_1,t')|V(\mathbf{r})|\psi_\alpha(t_1,t')\rangle dt_1. \tag{C14}$$

Next, we consider a scattering phenomenon when a electron scatters from a known t-t'-Floquet state $|\psi_\beta(t,t')\rangle$ into a distinct t-t'-Floquet state $|\Psi_\alpha(t,t')\rangle$ with a constant quasienergy ε as follows:

$$|\psi_\beta(t,t')\rangle = \exp\left(-\frac{i}{\hbar}\varepsilon_\beta t\right)|\phi_\beta(t')\rangle \xrightarrow{\text{scattering}} |\Psi_\alpha(t,t')\rangle = \exp\left(-\frac{i}{\hbar}\varepsilon t\right)|\Phi_\alpha(t')\rangle. \tag{C15}$$

This phenomenon is illustrated in Fig. 6. We can calculate the scattering amplitude for this scattering scenario using the

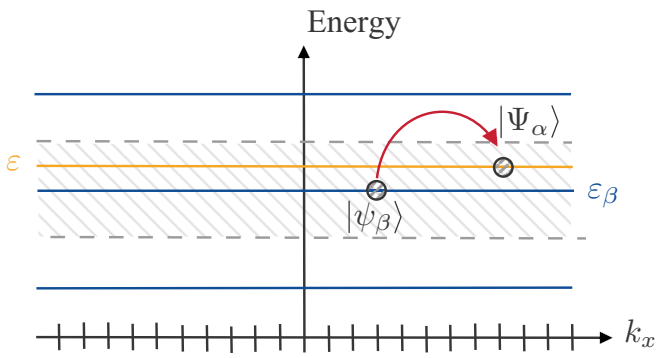

FIG. 6. Scattering from known $|\psi_\beta(t,t')\rangle$ state to a constant energy state $|\Psi_\alpha(t,t')\rangle$ due to the scattering potential created by impurities in the material.

expression derived in Eq. (C14) as follows:

$$a_{\alpha\beta}(t,t') = -\frac{i}{\hbar}\int_0^t e^{\frac{i}{\hbar}(\varepsilon_\beta-\varepsilon)t_1}\langle\phi_\beta(t')|V(\mathbf{r})|\phi_\alpha(t')\rangle dt_1. \quad \text{(C16)}$$

By assuming for a long duration ($t\to\infty$), we can turn this integral into a delta distribution

$$a_{\alpha\beta}(t') = -2\pi i\delta(\varepsilon_\beta-\varepsilon)Q, \quad \text{(C17)}$$

where $Q = \langle\phi_\beta(t')|V(\mathbf{r})|\phi_\alpha(t')\rangle$ and using the completeness properties we can rewrite this as

$$Q = \sum_{\mathbf{k}}\sum_{\mathbf{k}'}\langle\phi_\beta(t')|\mathbf{k}'\rangle\langle\mathbf{k}'|V(\mathbf{r})|\mathbf{k}\rangle\langle\mathbf{k}|\phi_\alpha(t')\rangle. \quad \text{(C18)}$$

Moreover, separating x-directional and y-directional momentum components, we can simply this to obtain

$$Q = \sum_{k_x}\sum_{k'_x}\int_{-\infty}^{\infty}\int_{-\infty}^{\infty}V_{\mathbf{k}',\mathbf{k}}\phi^\dagger_\beta(\mathbf{k}',t')\phi_\alpha(\mathbf{k},t')dk_y dk'_y, \quad \text{(C19)}$$

with $V_{\mathbf{k}',\mathbf{k}} = \langle\mathbf{k}'|V(\mathbf{r})|\mathbf{k}\rangle$.

Since we are presenting the perturbation potential $V(\mathbf{r})$ by a group of randomly distributed impurities, we take into account N_{imp} number of identical single impurity potentials distributed at randomly but in fixed positions $\mathbf{r}_i$. Thus we can describe the scattering potential $V(\mathbf{r})$ as the sum of uncorrelated single impurity potentials $\upsilon(\mathbf{r})$

$$V(\mathbf{r}) = \sum_{i=1}^{N_{\text{imp}}}\upsilon(\mathbf{r}-\mathbf{r}_i). \quad \text{(C20)}$$

Furthermore, we model the perturbation $V(\mathbf{r})$ as a Gaussian random potential where one can choose the zero of energy such that the potential is zero on average. This model is characterized by the following two equations [69]:

$$\langle\upsilon(\mathbf{r})\rangle_{\text{imp}} = 0, \quad \text{(C21a)}$$

$$\langle\upsilon(\mathbf{r})\upsilon(\mathbf{r}')\rangle_{\text{imp}} = \Upsilon(\mathbf{r}-\mathbf{r}'), \quad \text{(C21b)}$$

where $\langle\cdot\rangle_{\text{imp}}$ represents the average over the impurity disorder and $\Upsilon(\mathbf{r}-\mathbf{r}')$ is any decaying function depends only on $\mathbf{r}-\mathbf{r}'$. In addition, this model assumes that $\upsilon(\mathbf{r}-\mathbf{r}')$ only depends on the magnitude of the position difference $|\mathbf{r}-\mathbf{r}'|$, and it decays with a characteristic length r_c. Since this study considers the case where the wavelength of radiation or scattering electron is much greater than r_c, it is a better approximation to make two-point correlation function to be

$$\langle\upsilon(\mathbf{r})\upsilon(\mathbf{r}')\rangle_{\text{imp}} = \Upsilon^2_{\text{imp}}\delta(\mathbf{r}-\mathbf{r}'), \quad \text{(C22)}$$

where Υ^2_{imp} is a constant. A random potential $V(\mathbf{r})$ with this property is called white noise [69]. Then we can approximately model the total scattering potential as

$$V(\mathbf{r}) = \sum_{i=1}^{N_{\text{imp}}}\Upsilon_{\text{imp}}\delta(\mathbf{r}-\mathbf{r}_i). \quad \text{(C23)}$$

Here we can identify the Υ_{imp} as the strength of the delta potential. Furthermore, we can calculate $V_{\mathbf{k}',\mathbf{k}}$ using this assumption as follows:

$$V_{\mathbf{k}',\mathbf{k}} = \langle\mathbf{k}'|\sum_{i=1}^{N_{\text{imp}}}\Upsilon_{\text{imp}}\delta(\mathbf{r}-\mathbf{r}_i)|\mathbf{k}\rangle \quad \text{(C24a)}$$

$$= \sum_{i=1}^{N_{\text{imp}}}\int_{-\infty}^{\infty}\left[\frac{1}{\sqrt{L_xL_y}}e^{ik'_y y}\delta(y-y_i)\right.$$
$$\left.\times\frac{1}{\sqrt{L_xL_y}}e^{-ik_y y}\langle k'_x|\Upsilon_{\text{imp}}\delta(x-x_i)|k_x\rangle\right]dy \quad \text{(C24b)}$$

$$= \sum_{i=1}^{N_{\text{imp}}}\frac{1}{L_xL_y}e^{i(k'_y-k_y)y}\langle k'_x|\Upsilon_{\text{imp}}\delta(x-x_i)|k_x\rangle. \quad \text{(C24c)}$$

Since $\upsilon(\mathbf{r})$ in momentum space is a constant value, each impurity produce same impurity potential for every x-directional momentum pairs. Additionally, assuming the total number of scatters N_{imp} is microscopically large, we can derive

$$V_{\mathbf{k}',\mathbf{k}} = V_{k'_x,k_x}\frac{N_{\text{imp}}}{L_yL_x}\int_{-\infty}^{\infty}e^{i(k'_y-k_y)y_i}dy_i \quad \text{(C25a)}$$

$$= \eta_{\text{imp}}V_{k'_x,k_x}\delta(k'_y-k_y). \quad \text{(C25b)}$$

In the above equation, we introduced

$$V_{k'_x,k_x} = \langle k'_x|\Upsilon_{\text{imp}}\delta(x-x_i)|k_x\rangle, \quad \text{(C26)}$$

which is a constant value for every i impurity. Moreover, η_{imp} is the number of impurities in a unit area. It is important to note that in the above expression $\langle x|k_x\rangle = e^{-ik_x x}$.

Now using Eqs. (10) and (C25b) on Eq. (C19), we obtain

$$Q = \sum_{k_x}\sum_{k'_x}\eta_{\text{imp}}V_{k'_x,k_x}L_x\int_{-\infty}^{\infty}\int_{-\infty}^{\infty}\delta(k'_y-k_y)$$
$$\times\widetilde{\chi}_{n_\beta}(k'_y-b\cos(\omega t))\widetilde{\chi}_{n_\alpha}(k_y-b\cos(\omega t))$$
$$\times e^{i[k'_y-k_y]d\sin(\omega t)}e^{i[k'_y y'_0-k_y y_0]}dk'_y dk_y. \quad \text{(C27)}$$

Here we have changed the time variable $t' \to t$ only for the simplicity of notation. We can more simply this as

$$Q = \sum_{k_x} \sum_{k'_x} \eta_{\text{imp}} L_x V_{k'_x,k_x} I, \tag{C28}$$

with

$$I = \int_{-\infty}^{\infty} \widetilde{\chi}_{n_\beta}(k_y - b\cos(\omega t))\widetilde{\chi}_{n_\alpha}(k_y - b\cos(\omega t)) \times \exp(-ik_y(y_0 - y'_0))dk_y. \tag{C29}$$

To avoid the energy exchange from the dressing field and electrons in Landau levels, the applied radiation must be a purely dressing field. Therefore, in this study, we assume that the dressing field can only renormalize the probability of electron scattering inside a same Landau energy level ($n_\alpha = n_\beta = N$). This transform the Eq. (C29) to

$$I = \int_{-\infty}^{\infty} \widetilde{\chi}_N^2(k_y - b\cos(\omega t))\exp(-ik_y(y_0 - y'_0))dk_y. \tag{C30}$$

Using the Fourier transform of Gauss-Hermite functions [100] and the convolution theorem [101,102], we obtain

$$I = 2\pi \exp(b(y'_0 - y_0)\cos(\omega t)) \times \int_{-\infty}^{\infty} \chi_N(y)\chi_N(y_0 - y'_0 - y)dy. \tag{C31}$$

Finally, we can evaluate the scattering amplitude derived in Eq. (C17) for given $k_x = 2\pi m_\alpha/L_x$ and $k'_x = 2\pi m_\beta/L_x$ as follows:

$$a_{\alpha\beta}(k_x, k'_x, t) = -2\pi i \eta_{\text{imp}} L_x V_{k'_x,k_x} e^{b(y'_0 - y_0)\cos(\omega t)} \times \delta(\varepsilon_N - \varepsilon) \int_{-\infty}^{\infty} \chi_N(y)\chi_N(y_0 - y'_0 - y)dy. \tag{C32}$$

Since this scattering amplitude is time-periodic, we can write this as a Fourier series expansion

$$a_{\alpha\beta}(k_x, k'_x, t) = \sum_{l=-\infty}^{\infty} a^l_{\alpha\beta}(k_x, k'_x)e^{-il\omega t}. \tag{C33}$$

In addition, using the Jacobi-Anger expansion [103,104]

$$e^{iz\cos(\theta)} = \sum_{l=-\infty}^{\infty} i^l J_l(z)e^{-il\theta}, \tag{C34}$$

where $J_l(\cdot)$ are Bessel functions of the first kind with l integer order, we can rewrite the Eq. (C32) as follows:

$$a_{\alpha\beta}(k_x, k'_x, t) = \sum_{l=-\infty}^{\infty} -2\pi i^{l+1} \eta_{\text{imp}} L_x V_{k'_x,k_x} J_l(b(y'_0 - y_0)) \times \delta(\varepsilon_N - \varepsilon) \int_{-\infty}^{\infty} \chi_N(y)\chi_N(y_0 - y'_0 - y)dy \times e^{-il\omega t}. \tag{C35}$$

Thus we can identify the Fourier series component of the scattering amplitude as

$$a^l_{\alpha\beta}(k_x, k'_x) = -2\pi i^{l+1} \eta_{\text{imp}} L_x V_{k'_x,k_x} \delta(\varepsilon_N - \varepsilon) J_l(b(y'_0 - y_0)) \times \int_{-\infty}^{\infty} \chi_N(y)\chi_N(y_0 - y'_0 - y)dy. \tag{C36}$$

Furthermore, we can define *transition probability matrix* as

$$(A_{\alpha\beta})^{l,l'} = a^l_{\alpha\beta}\left[a^{l'}_{\alpha\beta}\right]^*, \tag{C37}$$

and this becomes

$$(A_{\alpha\beta})^{l,l'}(k_x, k'_x) = (2\pi \eta_{\text{imp}} L_x V_{k'_x,k_x})^2 \delta^2(\varepsilon_N - \varepsilon) \times J_l(b(y'_0 - y_0))J_{l'}(b(y'_0 - y_0)) \times \left|\int_{-\infty}^{\infty} \chi_N(y)\chi_N(y_0 - y'_0 - y)dy\right|^2. \tag{C38}$$

Then describing the square of the delta distribution using the following interpretation [29,33]:

$$\delta^2(\varepsilon) = \delta(\varepsilon)\delta(0) = \frac{\delta(\varepsilon)}{2\pi\hbar}\int_{-t/2}^{t/2} e^{i0\times t'/\hbar}dt' = \frac{\delta(\varepsilon)t}{2\pi\hbar}, \tag{C39}$$

and executing the time derivation operation on each matrix element of transition probability matrix, we receive the *transition amplitude matrix* elements

$$\Gamma^{ll'}_{\alpha\beta}(k_x, k'_x) = \frac{2\pi\eta^2_{\text{imp}}L^2_x}{\hbar}|V_{k'_x,k_x}|^2\delta(\varepsilon_\beta - \varepsilon) \times J_l(b(y'_0 - y_0))J_{l'}(b(y'_0 - y_0)) \times \left|\int_{-\infty}^{\infty} \chi_N(y)\chi_N(y_0 - y'_0 - y)dy\right|^2. \tag{C40}$$

Additionally, the inverse scattering time matrix can be identified as the sum of all available momentum over the impurity averaged transition probability matrix element [34,71]

$$\left(\frac{1}{\tau(\varepsilon, k_x)}\right)^{ll'}_{\alpha\beta} = \frac{1}{L_x}\sum_{k'_x} \langle * \rangle * \Gamma^{ll'}_{\alpha\beta}(k'_x, k_x)_{\text{imp}}. \tag{C41}$$

Next, applying the one-dimensional momentum continuum limit $\sum_{k'_x} \longrightarrow L_x/2\pi \int dk'_x$, we can obtain

$$\left(\frac{1}{\tau(\varepsilon, k_x)}\right)^{ll'}_{\alpha\beta} = \frac{2\pi\eta^2_{\text{imp}}L^2_x}{\hbar}\frac{V_{\text{imp}}}{2\pi}\delta(\varepsilon_\beta - \varepsilon) \times \int_{-\infty}^{\infty}\left\{J_l\left(\frac{b\hbar}{eB}(k_x - k'_x)\right)J_{l'}\left(\frac{b\hbar}{eB}(k_x - k'_x)\right)\left|\int_{-\infty}^{\infty}\chi_N(y)\chi_N\left(\frac{\hbar}{eB}(k'_x - k_x) - y\right)dy\right|^2\right\}dk'_x. \tag{C42}$$

Here an impurity average of white noise potential allows to identify $\langle |V_{k'_x,k_x}|^2\rangle_{\text{imp}} = V_{\text{imp}}$. Finally, using substitutions $k'_x = k_1$ and $y = \hbar k_2/(eB)$, we can derive our expression for the inverse scattering time matrix for Nth Landau level as follows:

$$\left(\frac{1}{\tau(\varepsilon,k_x)}\right)_N^{ll'} = \frac{\eta_{\text{imp}}^2 L_x^2 \hbar V_{\text{imp}}}{e^2B^2}\delta(\varepsilon-\varepsilon_N) \times \int_{-\infty}^{\infty}\left\{J_l\left(\frac{b\hbar}{eB}(k_x-k_1)\right)J_{l'}\left(\frac{b\hbar}{eB}(k_x-k_1)\right)\left|\int_{-\infty}^{\infty}\chi_N\left(\frac{\hbar}{eB}k_2\right)\chi_N\left(\frac{\hbar}{eB}(k_1-k_x-k_2)\right)dk_2\right|^2\right\}dk_1. \quad \text{(C43)}$$

APPENDIX D: CURRENT OPERATORS FOR A DRESSED QUANTUM HALL SYSTEM

In this section, we derive the current density operator for the Nth Landau level in a dressed quantum Hall system. We already found the exact solution for the time-dependent Schrödinger equation with the Hamiltonian give in Eq. (1) and we identified them as the Floquet states in Eq. (14). For the simplicity of notation, we can represent the Floquet modes derived in Eq. (10) as quantum states using their corresponding quantum numbers as follows:

$$|\phi_{n,m}\rangle = |n,k_x\rangle. \quad \text{(D1)}$$

Using this complete set of quantum states [34,36,64], we can represent the single-particle current operator's matrix element as

$$(\mathbf{j})_{nm,n'm'} = \langle n,k_x|\,\hat{\mathbf{j}}\,|n',k'_x\rangle. \quad \text{(D2)}$$

Next, we can identify the particle current operator for our system [59,60] as

$$\hat{\mathbf{j}} = \frac{1}{\widetilde{m}}\{\hat{\mathbf{p}} - e[\mathbf{A}_s + \mathbf{A}_d(t)]\}, \quad \text{(D3)}$$

where $\widetilde{m}$ is the mass of the considering particle.

First, we consider the x-directional particle current operator component, and we can identify that as

$$\hat{j}_x = \frac{1}{\widetilde{m}}\left(-i\hbar\frac{\partial}{\partial x} + eBy\right). \quad \text{(D4)}$$

Next, we calculate the matrix elements of x-directional current operator against our Floquet mode basis

$$(j_x)_{nm,n'm'} = \langle n,k_x|\,\frac{1}{\widetilde{m}}\left(-i\hbar\frac{\partial}{\partial x} + eBy\right)|n',k'_x\rangle, \quad \text{(D5)}$$

and we evaluate these using the Floquet modes derived in Eq. (7) as follows:

$$(j_x)_{nm,n'm'} = \frac{1}{\widetilde{m}}\delta_{k_x,k'_x}\int(\hbar k'_x + eBy) \times \chi_n(y-y_0-\zeta(t))\chi_{n'}(y-y_0-\zeta(t))dy. \quad \text{(D6)}$$

Let $[y-y_0-\zeta(t)] = \bar{y}$, and we can obtain

$$(j_x)_{nm,n'm'} = \frac{1}{\widetilde{m}}\delta_{k_x,k'_x}\int[\hbar k'_x + eB\bar{y} - \hbar k'_x + eB\zeta(t)] \times \chi_n(\bar{y})\chi_{n'}(\bar{y})d\bar{y}. \quad \text{(D7)}$$

Using the following integral identities of the Floquet modes that are made of Gauss-Hermite functions [105–107]

$$\int\chi_n(y)\chi_{n'}(y)dy = \delta_{n',n}, \quad \text{(D8)}$$

$$\int y\chi_n(y)\chi_{n'}(y)dy = \frac{1}{\kappa}\left(\sqrt{\frac{n+1}{2}}\delta_{n',n+1} + \sqrt{\frac{n}{2}}\delta_{n',n-1}\right), \quad \text{(D9)}$$

we simplify the matrix elements of x-directional current operator to obtain

$$(j_x)_{nm,n'm'} = \frac{eB}{\widetilde{m}\kappa}\delta_{k_x,k'_x} \times\left[\left(\sqrt{\frac{n+1}{2}}\delta_{n',n+1} + \sqrt{\frac{n}{2}}\delta_{n',n-1}\right) + \zeta(t)\delta_{n',n}\right]. \quad \text{(D10)}$$

Due to high complexity of extract solution, in this study we only consider the constant contribution from the Fourier series components of the above expression. Therefore we can identify the zeroth component of the Fourier series as

$$(j_x)_{nm,n'm'} = \frac{eB}{\widetilde{m}\kappa}\delta_{k_x,k'_x}\left(\sqrt{\frac{n+1}{2}}\delta_{n',n+1} + \sqrt{\frac{n}{2}}\delta_{n',n-1}\right). \quad \text{(D11)}$$

To calculate the electric current operator, we substitute the electron's charge and effective mass to the above derived equation. This leads to

$$\left(j^x_{s=0}\right)^{\text{electron}}_{nm,n'm'} = \frac{e\hbar}{m_e l_0}\delta_{k_x,k'_x}\left(\sqrt{\frac{n+1}{2}}\delta_{n',n+1} + \sqrt{\frac{n}{2}}\delta_{n',n-1}\right), \quad \text{(D12)}$$

where $l_0 = \sqrt{\hbar/eB}$ is the magnetic length.

Moreover, we can identify the y-directional current operator component as

$$\hat{j}_y = \frac{1}{\widetilde{m}}\left(-i\hbar\frac{\partial}{\partial y} - \frac{eE}{\omega}\cos(\omega t)\right). \quad \text{(D13)}$$

Using this operator, we can represent the matrix elements of y-directional current operator in Floquet mode basis as

$$(j_y)_{nm,n'm'} = \langle n, k_x| \frac{-1}{\widetilde{m}}\left(i\hbar\frac{\partial}{\partial y} + \frac{eE}{\omega}\cos(\omega t)\right)|n', k'_x\rangle. \tag{D14}$$

After following the same steps done for the x-directional current operator, and recursion relation of the first derivative of Gauss-Hermite functions [107]

$$\frac{\partial \chi_n(y)}{\partial y} = \kappa\left[-\sqrt{\frac{n+1}{2}}\chi_{n+1}(y) + \sqrt{\frac{n}{2}}\chi_{n-1}(y)\right], \tag{D15}$$

we can identify the zeroth component of matrix elements for y-directional electric current operator as

$$\left(j^y_{s=0}\right)^{\text{electron}}_{nm,n'm'} = \frac{ie\hbar\kappa}{m_e}\delta_{k_x,k'_x}\left(\sqrt{\frac{n}{2}}\delta_{n',n-1} - \sqrt{\frac{n+1}{2}}\delta_{n',n+1}\right) \tag{D16}$$

and

$$\left(j^y_{s=0}\right)^{\text{electron}}_{nm,n'm'} = \frac{ie\hbar}{m_e l_0}\delta_{k_x,k'_x}\left(\sqrt{\frac{n}{2}}\delta_{n',n-1} - \sqrt{\frac{n+1}{2}}\delta_{n',n+1}\right). \tag{D17}$$

[1] Y. Liu, N. O. Weiss, X. Duan, H. C. Cheng, Y. Huang, and X. Duan, Nat. Rev. Mater. **1**, 16042 (2016).
[2] R. T. Wijesekara, S. D. Gunapala, M. I. Stockman, and M. Premaratne, Phys. Rev. B **101**, 245402 (2020).
[3] L. Tao, Z. Chen, Z. Li, J. Wang, X. Xu, and J.-B. Xu, InfoMat **3**, 36 (2020).
[4] R. T. Wijesekara, S. D. Gunapala, and M. Premaratne, Phys. Rev. B **104**, 045405 (2021).
[5] D. Rodrigo, O. Limaj, D. Janner, D. Etezadi, F. J. G. De Abajo, V. Pruneri, and H. Altug, Science **349**, 165 (2015).
[6] S. Pirandola, B. R. Bardhan, T. Gehring, C. Weedbrook, and S. Lloyd, Nat. Photoics **12**, 724 (2018).
[7] H. Hapuarachchi, S. Mallawaarachchi, H. T. Hattori, W. Zhu, and M. Premaratne, J. Phys.: Condens. Matter **30**, 054006 (2018).
[8] D. Weeraddana, M. Premaratne, and D. L. Andrews, Phys. Rev. B **92**, 035128 (2015).
[9] M. Yuan, M. Liu, and E. H. Sargent, Nat. Energy **1**, 16016 (2016).
[10] B. Sun, O. Ouellette, F. P. G. de Arquer, O. Voznyy, Y. Kim, M. Wei, A. H. Proppe, M. I. Saidaminov, J. Xu, M. Liu *et al.*, Nat. Commun. **9**, 4003 (2018).
[11] J. Huh, G. G. Guerreschi, B. Peropadre, J. R. McClean, and A. Aspuru-Guzik, Nat. Photonics **9**, 615 (2015).
[12] S. Slussarenko and G. J. Pryde, Appl. Phys. Rev. **6**, 041303 (2019).
[13] U. L. Andersen, Nature (London) **591**, 40 (2021).
[14] A. Marais, B. Adams, A. K. Ringsmuth, M. Ferretti, J. M. Gruber, R. Hendrikx, M. Schuld, S. L. Smith, I. Sinayskiy, T. P. Krüger *et al.*, J. R. Soc., Interface **15**, 20180640 (2018).
[15] F. Bian, L. Sun, L. Cai, Y. Wang, and Y. Zhao, Proc. Natl. Acad. Sci. USA **117**, 22736 (2020).
[16] N. Rivera and I. Kaminer, Nat. Rev. Phys. **2**, 538 (2020).
[17] V. M. Shalaev, Nat. Photonics **1**, 41 (2007).
[18] K. J. Si, D. Sikdar, Y. Chen, F. Eftekhari, Z. Xu, Y. Tang, W. Xiong, P. Guo, S. Zhang, Y. Lu *et al.*, ACS Nano **8**, 11086 (2014).
[19] H. Hapuarachchi, S. D. Gunapala, and M. Premaratne, J. Phys.: Condens. Matter **31**, 325301 (2019).
[20] T. Perera, S. D. Gunapala, M. I. Stockman, and M. Premaratne, J. Phys. Chem. C **124**, 27694 (2020).
[21] W. W. Chow and F. Jahnke, Prog. Quantum Electron. **37**, 109 (2013).
[22] C. Jayasekara, M. Premaratne, S. D. Gunapala, and M. I. Stockman, J. Appl. Phys. **119**, 133101 (2016).
[23] M. Premaratne and M. I. Stockman, Adv. Opt. Photonics **9**, 79 (2017).
[24] M. Tsang, Phys. Rev. A **81**, 063837 (2010).
[25] B. Liu, W. Zhu, S. D. Gunapala, M. I. Stockman, and M. Premaratne, ACS Nano **11**, 12573 (2017).
[26] A. Devi, S. D. Gunapala, M. I. Stockman, and M. Premaratne, Phys. Rev. A **102**, 013701 (2020).
[27] T. Kitagawa, T. Oka, A. Brataas, L. Fu, and E. Demler, Phys. Rev. B **84**, 235108 (2011).
[28] Y. Zhou and M. W. Wu, Phys. Rev. B **83**, 245436 (2011).
[29] O. V. Kibis, Europhys. Lett. **107**, 57003 (2014).
[30] A. A. Pervishko, O. V. Kibis, S. Morina, and I. A. Shelykh, Phys. Rev. B **92**, 205403 (2015).
[31] S. Morina, O. V. Kibis, A. A. Pervishko, and I. A. Shelykh, Phys. Rev. B **91**, 155312 (2015).
[32] H. Dehghani, T. Oka, and A. Mitra, Phys. Rev. B **91**, 155422 (2015).
[33] K. Dini, O. V. Kibis, and I. A. Shelykh, Phys. Rev. B **93**, 235411 (2016).
[34] M. Wackerl, P. Wenk, and J. Schliemann, Phys. Rev. B **101**, 184204 (2020).
[35] M. Premaratne and G. P. Agrawal, *Theoretical Foundations of Nanoscale Quantum Devices* (Cambridge University Press, 2021).
[36] M. Grifoni and P. Hänggi, Phys. Rep. **304**, 229 (1998).
[37] C. Cohen-Tannoudji, J. Dupont-Roc, and G. Grynberg, *Atom—Photon Interactions* (Wiley, 1998).
[38] M. Scully and M. Zubairy, *Introduction to Quantum Optics* (Cambridge University Press, 2001).
[39] S. Girvin and R. Prange, *The quantum Hall effect* (Springer-Verlag, New York, 1990).
[40] T. Ando, Y. Matsumoto, Y. Uemura, M. Kobayashi, and K. F. Komatsubara, J. Phys. Soc. Jpn. **32**, 859 (1972).
[41] T. Ando and Y. Uemura, J. Phys. Soc. Jpn. **36**, 959 (1974).
[42] T. Ando, J. Phys. Soc. Jpn. **36**, 1521 (1974).
[43] T. Ando, J. Phys. Soc. Jpn. **37**, 622 (1974).
[44] T. Ando and Y. Uemura, J. Phys. Soc. Jpn. **37**, 1233 (1974).
[45] T. Ando, A. B. Fowler, and F. Stern, Rev. Mod. Phys. **54**, 437 (1982).
[46] A. Endo, N. Hatano, H. Nakamura, and R. Shirasaki, J. Phys.: Condens. Matter **21**, 345803 (2009).

[47] A. Allerman, W. Xu, N. Hauser, and C. Jagadish, J. Appl. Phys. **77**, 2052 (1995).
[48] B. Tieke, R. Fletcher, U. Zeitler, A. K. Geim, M. Henini, and J. C. Maan, Phys. Rev. Lett. **78**, 4621 (1997).
[49] W. Pan, J. S. Xia, H. L. Stormer, D. C. Tsui, C. L. Vicente, E. D. Adams, N. S. Sullivan, L. N. Pfeiffer, K. W. Baldwin, and K. W. West, Phys. Rev. Lett. **95**, 066808 (2005).
[50] M. A. Zudov, R. R. Du, J. A. Simmons, and J. L. Reno, Phys. Rev. B **64**, 201311(R) (2001).
[51] R. G. Mani, J. H. Smet, K. von Klitzing, V. Narayanamurti, W. B. Johnson, and V. Umansky, Nature (London) **420**, 646 (2002).
[52] M. A. Zudov, R. R. Du, L. N. Pfeiffer, and K. W. West, Phys. Rev. Lett. **90**, 046807 (2003).
[53] R. G. Mani, J. H. Smet, K. von Klitzing, V. Narayanamurti, W. B. Johnson, and V. Umansky, Phys. Rev. Lett. **92**, 146801 (2004).
[54] A. C. Durst, S. Sachdev, N. Read, and S. M. Girvin, Phys. Rev. Lett. **91**, 086803 (2003).
[55] I. A. Dmitriev, A. D. Mirlin, and D. G. Polyakov, Phys. Rev. Lett. **91**, 226802 (2003).
[56] I. A. Dmitriev, M. G. Vavilov, I. L. Aleiner, A. D. Mirlin, and D. G. Polyakov, Phys. Rev. B **71**, 115316 (2005).
[57] I. A. Dmitriev, M. Khodas, A. D. Mirlin, D. G. Polyakov, and M. G. Vavilov, Phys. Rev. B **80**, 165327 (2009).
[58] L. Landau, Z. Phys. **64**, 629 (1930).
[59] G. D. Mahan, *Many-Particle Physics* (Springer Science & Business Media, New York, 2000).
[60] H. Bruus and K. Flensberg, *Many-Body Quantum Theory in Condensed Matter Physics: An Introduction* (Oxford University Press, New York, 2004).
[61] K. Husimi, Prog. Theor. Phys. **9**, 381 (1953).
[62] T. Dittrich, P. HÃ¤nggi, G. L. Ingold, B. Kramer, G. Schön, and W. Zwerger, *Quantum Transport and Dissipation* (Wiley-VCH, Weinheim, 1998).
[63] G. Floquet, Scientific annals of the École Normale Supérieure **12**, 47 (1883).
[64] M. Holthaus, J. Phys. B: At., Mol. Opt. Phys. **49**, 013001 (2015).
[65] V. Popov and A. Perelomov, J. Exp. Theor. Phys. **30**, 910 (1970).
[66] H. Sambe, Phys. Rev. A **7**, 2203 (1975).
[67] U. Peskin, R. Kosloff, and N. Moiseyev, J. Chem. Phys. **100**, 8849 (1994).
[68] S. C. Althorpe, D. J. Kouri, D. K. Hoffman, and N. Moiseyev, Chem. Phys. **217**, 289 (1997).
[69] E. Akkermans and G. Montambaux, *Mesoscopic Physics of Electrons and Photons* (Cambridge University Press, 2010).
[70] R. Winkler, *Spin-orbit Coupling Effects in Two-Dimensional Electron and Hole Systems* (Springer, Berlin, 2003).
[71] M. Wackerl, *Ph.D. thesis*, University of Regensburg, 2020.
[72] N. Tsuji, T. Oka, and H. Aoki, Phys. Rev. B **78**, 235124 (2008).
[73] K. I. Seetharam, C.-E. Bardyn, N. H. Lindner, M. S. Rudner, and G. Refael, Phys. Rev. B **99**, 014307 (2019).
[74] M. S. Rudner and N. H. Lindner, Nat. Rev. Phys. **2**, 229 (2020).
[75] N. H. Lindner, E. Berg, and M. S. Rudner, Phys. Rev. X **7**, 011018 (2017).
[76] M. Bukov, L. D'Alessio, and A. Polkovnikov, Adv. Phys. **64**, 139 (2015).
[77] A. Eckardt and E. Anisimovas, New J. Phys. **17**, 093039 (2015).
[78] T. Kuwahara, T. Mori, and K. Saito, Ann. Phys. **367**, 96 (2016).
[79] D. A. Abanin, W. De Roeck, W. W. Ho, and F. Huveneers, Phys. Rev. B **95**, 014112 (2017).
[80] T. Mori, T. N. Ikeda, E. Kaminishi, and M. Ueda, J. Phys. B: At. Mol. Opt. Phys. **51**, 112001 (2018).
[81] See Supplemental Material at http://link.aps.org/supplemental/10.1103/PhysRevB.xx.xxxxxx for complete numerical simulations of the longitudinal conductivity in dressed quantum Hall system.
[82] J. Wakabayashi and S. Kawaji, J. Phys. Soc. Jpn. **44**, 1839 (1978).
[83] Y. Ochiai, M. Mizuno, M. Kawabe, K. Ishibashi, Y. Aoyagi, K. Gamo, and S. Namba, Jpn. J. Appl. Phys. **29**, L739 (1990).
[84] F. B. Mancoff, L. J. Zielinski, C. M. Marcus, K. Campman, and A. C. Gossard, Phys. Rev. B **53**, R7599 (1996).
[85] Y. G. Arapov, G. Alshanskii, G. Harus, V. Neverov, N. Shelushinina, M. Yakunin, and O. Kuznetsov, Nanotechnology **13**, 86 (2002).
[86] B. Grbić, C. Ellenberger, T. Ihn, K. Ensslin, D. Reuter, and A. Wieck, Appl. Phys. Lett. **85**, 2277 (2004).
[87] A. D. Caviglia, S. Gariglio, C. Cancellieri, B. Sacépé, A. Fete, N. Reyren, M. Gabay, A. F. Morpurgo, and J.-M. Triscone, Phys. Rev. Lett. **105**, 236802 (2010).
[88] A. B. Fowler, F. F. Fang, W. E. Howard, and P. J. Stiles, Phys. Rev. Lett. **16**, 901 (1966).
[89] K. V. Klitzing, G. Dorda, and M. Pepper, Phys. Rev. Lett. **45**, 494 (1980).
[90] T. Ando and Y. Murayama, J. Phys. Soc. Jpn. **54**, 1519 (1985).
[91] O. E. Dial, R. C. Ashoori, L. N. Pfeiffer, and K. W. West, Nature (London) **448**, 176 (2007).
[92] C. H. Ahn, J. M. Triscone, and J. Mannhart, Nature (London) **424**, 1015 (2003).
[93] Y. Deng, Y. Yu, Y. Song, J. Zhang, N. Z. Wang, Z. Sun, Y. Yi, Y. Z. Wu, S. Wu, J. Zhu *et al.*, Nature (London) **563**, 94 (2018).
[94] F. Yang, Z. Zhang, N. Z. Wang, G. J. Ye, W. Lou, X. Zhou, K. Watanabe, T. Taniguchi, K. Chang, X. H. Chen *et al.*, Nano Lett. **18**, 6611 (2018).
[95] G. Long, X. Chen, S. Xu, and N. Wang, in *Hybrid Nanomaterials-Flexible Electronics Materials* (IntechOpen, 2020).
[96] L. Li, Y. Yu, G. J. Ye, Q. Ge, X. Ou, H. Wu, D. Feng, X. H. Chen, and Y. Zhang, Nat. Nanotechnol. **9**, 372 (2014).
[97] K. Hirakawa, K. Yamanaka, M. Endo, M. Saeki, and S. Komiyama, Phys. Rev. B **63**, 085320 (2001).
[98] D. J. Griffiths and D. F. Schroeter, *Introduction to Quantum Mechanics* (Cambridge University Press, 2018).
[99] R. Shankar, *Principles of Quantum Mechanics* (Springer, New York, 1994).
[100] E. Celeghini, M. Gadella, and M. A. del Olmo, Symmetry **13**, 853 (2021).
[101] G. Arfken, *Mathematical Methods for Physicists* (Academic, San Diego, 1985).
[102] R. Bracewell, *The Fourier Transform and Its Applications* (McGraw-Hill, New York, 1978).

[103] A. Cuyt, V. Petersen, B. Verdonk, H. Waadeland, and W. Jones, *Handbook of Continued Fractions for Special Functions* (Springer, Dordrecht, 2008).

[104] M. Abramowitz and I. A. Stegun, *Handbook of Mathematical Functions with Formulas, Graphs, and Mathematical Tables* (Dover, New York, 1964).

[105] V. Vedenyapin, A. Sinitsyn, and E. Dulov, *Kinetic Boltzmann, Vlasov and Related Equations* (Elsevier, Amsterdam, 2011).

[106] G. Szegö, *Orthogonal Polynomials* (American Mathematical Society, New York, 1959).

[107] J. P. Boyd, *Dynamics of the Equatorial Ocean* (Springer, 2018).